

# **Evaluation of Seismic Performance of Reinforced Concrete Buildings Using Incremental Dynamic Analysis (IDA) for Near Field Earthquakes**

**Hassan Moniri**

Submitted to the  
Institute of Graduate Studies and Research  
in partial fulfilment of the requirements for the Degree of

Master of Science  
in  
Civil Engineering

Eastern Mediterranean University  
October 2014  
Gazimağusa, North Cyprus

Approval of the Institute of Graduate Studies and Research

---

Prof. Dr. Elvan Yılmaz  
Director

I certify that this thesis satisfies the requirements as a thesis for the degree of Master of Science in Civil Engineering.

---

Prof. Dr. Özgür Eren  
Chair, Department of Civil Engineering

We certify that we have read this thesis and that in our opinion it is fully adequate in scope and quality as a thesis for the degree of Master of Science in Civil Engineering.

---

Asst. Prof. Dr. Serhan Şensoy  
Supervisor

---

Examining Committee

1. Asst. Prof. Dr. Mürüde Çelikağ

---

2. Asst. Prof. Dr. Giray Ozay

---

3. Asst. Prof. Dr. Serhan Şensoy

---

## ABSTRACT

In the proximity of an active fault system, ground motions are significantly affected by the faulting mechanism, direction of rupture propagation relative to the site (e.g., forward directivity), as well as the possible static deformation of the ground surface associated with fling-step effects. These near-source outcomes cause most of the seismic energy from the rupture to arrive in a single coherent long-period pulse of motion. Failures of modern engineered structures observed within the near-fault region in 1994 Northridge earthquake revealed the vulnerability of existing buildings against pulse-type ground motions. Additionally, strong directivity effects during the 1999 Kocaeli, Duzce, and Chi-Chi earthquakes renewed attention on the consequences of near-fault ground motions on structures. Hence, the relevant question becomes how vulnerable is the present structure to near fault ground motions, whereas they were designed for far faults ground motions.

This thesis investigates the results of illustrious characteristics of near-fault ground motions on the seismic response of three reinforced concrete structures (6-Story, 10-Story and 15-Story). The structures are designed in compliance with the ACI code specification and ground motion was scaled according to ASCE 07-05 standard to apply in nonlinear time history analysis. Preliminary design of models is carried out by using ETABS software and the nonlinear structural evaluations are carried out by using the OpenSees software.

Numerical modelling carried out in this thesis showed that the reinforced concrete buildings are under large deformation requirements during the presence of velocity pulses in velocity time history. Incremental dynamic analysis (IDA) solutions revealed that considerable amount of energy is required to be wasted and reach to collapse point. Moreover, result of this study shows that the vertical pulse of ground motion can be illustrious influence on seismic response of building when it combined with horizontal pulse.

**Keywords:** Near-fault, Reinforced concrete building, Fling step, Incremental dynamic analysis (IDA), Seismic demands.

## ÖZ

Aktif fay hattı yakınında oluşan yer hareketleri faylanma mekanizmasının çeşidi, bulunulan konuma göre yırtılma yönü (örneğin ileri atımlı faylanma) ve de ani atılımdan dolayı yer kabuğunda oluşan deformasyona göre ciddi farklılıklar içermektedir. Faylanma yakınında sismik enerjinin büyük bir bölümü ahenkli uzun periyotlu daarbeli bir titreşime neden olmaktadır. Yakın zamanda, özellikle 1994 Northridge depreminde yakın fay hattının neden olduğu darbeli titreşimler nedeniyle mühendislik hizmeti görmüş modern yapıların dahi savunmasız olduğunu göstermiştir. Buna ilaveten 1999 Kocaeli, Düzce ve Chi-Chi depremleri de yakın fay hatlarının yapılara etkisi konusunun gündeme getirmiştir. Burada sorulması gereken soru uzak bölgede oluşan depremin etkileri kullanılarak tasarlanmış mevcut yapıların yakın bölge depremlerinin neden oldu etki altında ne kadar savunmasız olduklarıdır.

Bu tezde 6, 10, 15 katlı betonarme yapıların yakın faylanma nedeniyle oluşan deprem titreşimi ve ani hareketleri karşısında davranışları incelenmiştir. Bu amaçla oluşturulan çerçeve modeller önce ACI-318 yönetmeliği esas alınarak tasarlanmış ve zaman tanım alanında doğrusal olmayan analiz için ise ASCE 07-05 yöntemi (yöntemi) doğrultusunda deprem kayıtları ölçeklendirilmiştir. Modellerin tasarımı ETABS yazılımı ve zaman tanım alanında doğrusal olmayan analiz için ise OpenSees yazılımı kullanılmıştır.

Bu çalışma doğrultusunda yapılan analizler neticesinde, betonarme yapıların hız zaman tanımı altında, özellikle ani hız atılımının olduğu durumlarda deformasyon

talebinin büyük olacağı yönündedir. Artımsal Dinamik Analiz (IDA) sonuçları göstermiştir ki bu yapıların göçme durumuna gelebilmeleri için büyük boyutta enerji yutma kapasitesine ihtiyaç vardır. Öte yandan yakın fay bölgelerinde düşey yer hareketi etkisinin de özellikle yatay yer hareketi ile birlikte incelenmesi gerektiği sonucuna bu çalışma sınırları içerisinde ulaşılmıştır.

**Anahtar Kelimeler:** Yakın fay bölgesi, Betonarme yapılar, Fay deformasyonu, Artımsal Dinamik Analiz, Seismik talep.

# DEDICATION

*To My Supportive Father;*

*My Symbol of Strength*

*Who Offered Me Full Support in Life...*

*And My Affectionate Mother;*

*My Symbol of Patience*

*Who Taught Me the Life Alphabets...*

## **ACKNOWLEDGMENT**

My sincere appreciation goes to my honoured supervisor, Dr. Serhan Şensoy who spared no effort to me, and whose valuable suggestions with endless patience perpetually shed light on my path. I believe that without his help it would be really difficult to handle such a research.

I am also grateful to all those who taught me even a word, specially my lecturers at Civil Engineering Department of EMU who offered me expert advice.

My deepest and warmest appreciation goes to my lovely and caring family for their everlasting support, patience and thoughtfulness; my amicable parents who compassionately taught me how to live; my dear Mohammad, and my lovely sisters Fatemeh who made it all possible by their persistent encouragements.

I am also indebted to my dear friend, M. Abkenari, for her abundant moral supports in this whole time. I would also like to extend my special thanks to all of my dear friends and classmates, who supported me in writing, and motivated me to strive towards my goal.

# TABLE OF CONTENTS

ABSTRACT .....	iii
ÖZ .....	v
DEDICATION.....	vii
ACKNOWLEDGMENT .....	viii
LIST OF TABLES .....	xii
LIST OF FIGURES .....	xiii
LIST OF ABBREVIATIONS .....	xvi
LIST OF SYMBOLS .....	xviii
1 INTRODUCTION .....	1
1.1 Introduction .....	1
1.2 Methodology .....	3
1.3 Research Objectives .....	3
1.4 Thesis Overview.....	4
2 LITERATURE REVIEW.....	5
2.1 Introduction .....	5
2.2 Previous Research on Global Collapse.....	9
2.2.1 P- $\Delta$ effects.....	10
2.2.2 Degrading Hysteretic Models .....	11
2.2.3 Analytical Collapse Investigations.....	13
2.2.4 Evaluating the Expected Spectral Shape Effect on Collapse Assessment.....	14
2.2.5 Experimental Collapse Investigations.....	16
2.3 Description of Global Collapse Assessment Approach.....	18
2.3.1 Selection of Ground Motions.....	19

2.3.2 Deterioration Models.....	19
2.3.3 Structural Systems.....	20
2.3.4 Collapse Capacity .....	21
2.3.5 Effects of Uncertainty in System Parameters .....	22
2.4 Collapse Assessment of SDOF Systems.....	24
3 INCREMENTAL DYNAMIC ANALYSIS .....	26
3.1 Introduction .....	26
3.2 Fundamentals of Incremental Dynamic Analysis .....	31
3.2.1 Introduction .....	31
3.2.2 Fundamentals of Single-Record IDAs .....	33
3.2.3 Capacity and Limit-States on Single IDA Curves .....	36
3.2.4 Multi-Record IDAs and Their Summary.....	38
3.3 Operational Damage Levels.....	42
3.4 Confidence Level of Global Collapse .....	44
3.4.1 Median Drift Demand (D).....	45
3.4.2 Median Drift Capacity (C).....	45
3.4.3 Resistance Factor ( $\phi$ ).....	45
3.4.4 Determining the Slope of Hazard Curve (k).....	47
3.4.5 Determination of $\gamma$ .....	48
3.4.6 Determination of $\gamma a$ .....	49
3.4.7 Calculation of $\beta_{UT}$ .....	50
3.4.8 Calculation of Confidence Parameter ( $\lambda$ ).....	50
3.5 Construction of Fragility Curves.....	51
3.5.1 Overview of Fragility Curves .....	51
3.5.2 Uncertainties Effects on Fragility Curves .....	52

4 THE PROPOSED METHOD.....	54
4.1 Introduction.....	54
4.2 Buildings in the study.....	55
4.3 Performed analysis.....	58
4.4 Ground motion records and the analyses.....	59
5 RESULTS AND DISCUSSION OF THE RESULTS.....	64
5.1 Introduction.....	64
5.2 Ground motion records.....	65
5.3 Results extraction.....	65
5.4 Analyses results.....	66
5.4.1 IDA Curves.....	66
5.4.2 Storey model, far-fault & near-fault.....	73
5.5 Discussion.....	83
6 CONCLUSION AND RECOMMENDATIONS FOR FURTHER RESEARCH ..	86
6.1 Conclusion.....	86
6.2 Suggestions for Further Research.....	88
REFERENCES.....	89

## LIST OF TABLES

Table 3.1. Hazard level (SEAOC 2000) .....	42
Table 3.2. Hazard and operational levels ATC-40, FEMA-356.....	43
Table 4.1. Columns' and Beams' sections specifications .....	58
Table 4.2. Specifications of near-fault ground motion records.....	60
Table 4.3. Specifications of far-fault ground motion records .....	61
Table 5.1. Comparing the mean values of the maximum displacement under near- and far-field ground motion records (mm).....	77
Table 5.2. Comparing the mean values of the maximum inter-storey drift under near- and far-field ground motion records (mm).....	81

## LIST OF FIGURES

Figure 2.1. Model offered by Ibarra (2005) .....	12
Figure 2.2. Comparison of an observed spectrum from a Loma Prieta motion with spectra predicted by Boore et al. (1997); after Haselton and Baker (2006) .....	16
Figure 2.3. EDP curve, relative intensity (Vamvatsikos and Cornell, 2002).....	19
Figure 2.4. The response of an SDOF system represented by a peak-oriented model with rapid cyclic deterioration (Luis F. Ibarra and H. Krawinkler, 2004) .....	20
Figure 2.5. Different pushover curves for $(S_a/g) / \eta$ (Ibarra and Krawinkler, 2005) .....	22
Figure 2.6. Uncertainty in system parameters (Vamvatsikos, 2002).....	23
Figure 2.7. Effect of uncertainties on system parameters with different (Song, 2002) .....	23
Figure 3.1. Operational levels matrix (SEAOC 2000).....	43
Figure 3.2. Associated components involved in structural performance evaluation (Khanmohammadi, 2005) .....	44
Figure 4.1. Building models-Plan.....	57
Figure 4.2. Building models-Elevation view; a) 6-story b) 10-story c) 15-story .....	57
Figure 4.3. Far Faults ground motions were scaled to ASCE 7-05 standard. ....	62
Figure 4.4. Near Faults ground motions were scaled to ASCE 7-05 standard.....	62
Figure 4.5. Near Faults & Far Faults ground motions compare with ASCE 7-05 standard. ....	63

Figure 5.1. IDA curves and limit-state capacities for 6-story building: IDA curves for 14 far faults ground motions.....	67
Figure 5.2. The summary of IDA curves for 6-story building (Far fault ground motions).....	67
Figure 5.3. IDA curves and limit-state capacities for 6-storey building: IDA curves for 14 near faults ground motions.....	68
Figure 5.4. The summary of IDA curves for 6-story building (Near fault ground motions).....	68
Figure 5.5. IDA curves and limit-state capacities for 10-storey building: IDA curves for 14 far faults ground motions.....	69
Figure 5.6. The summary of IDA curves for 10-story building (Far fault ground motions).....	69
Figure 5.7. IDA curves and limit-state capacities for 10-storey building: IDA curves for 14 near faults ground motions.....	70
Figure 5.8. The summary of IDA curves for 10-story building (Near fault ground motions).....	70
Figure 5.9. IDA curves and limit-state capacities for 15-storey building: IDA curves for 14 far faults ground motions.....	71
Figure 5.10. The summary of IDA curves for 15-story building (Far fault ground motions).....	71
Figure 5.11. IDA curves and limit-state capacities for 15-storey building: IDA curves for 14 near faults ground motions.....	72
Figure 5.12. The summary of IDA curves for 15-story building (Near fault ground motions).....	72
Figure 5.13. Total displacement profile of 6-storey for far faults .....	74

Figure 5.14. Total displacement profile of 6-storey for near faults .....	74
Figure 5.15. Total displacement profile of 10-storey for far faults .....	75
Figure 5.16. Total displacement profile of 10-storey for near faults .....	75
Figure 5.17. Total displacement profile of 15-storey for far faults .....	76
Figure 5.18. Total displacement profile of 15-storey for near faults .....	76
Figure 5.19. Inter-Story Drift profile of 6-storey for far faults .....	78
Figure 5.20. Inter-Story Drift profile of 6-storey for near faults .....	78
Figure 5.21. Inter-Story Drift profile of 10-storey for far faults .....	79
Figure 5.22. Inter-Story Drift profile of 10-storey for near faults .....	79
Figure 5.23. Inter-Story Drift profile of 15-storey for far faults .....	80
Figure 5.24. Inter-Story Drift profile of 15-storey for near faults .....	80
Figure 5.25. Spectral velocity of the selected ground motion records for 6-story .....	82
Figure 5.26. Spectral velocity of the selected ground motion records for 10- story .....	82

## LIST OF ABBREVIATIONS

SDOF	Single Degree of Freedom
MDOF	Multi Degree of Freedom
IDA	Incremental Dynamic Analysis
RC	Reinforced Concrete
ICBO	International Conference of Building Officials
GM	Ground Motion
FEA	Finite Element Analysis
FEM	Finite Element Method
THA	Time History Analysis
EDPs	Engineering Demand Parameters
FOSM	First Order Second Moment
RTR	Record To Record variability
FEMA	Federal Emergency Management Agency
DPO	Dynamic Pushover
PBEE	Performance Based Earthquake Engineering
BSSC	Building Seismic Safety Council
SEAOC	Structural Engineers Association of California
USGS	U.S. Geological Survey
NEHRP	National Earthquake Hazards Reduction Program
UBC	Uniform Building Code
HAZUS	Hazards U.S.
NRHA	Nonlinear Response History Analysis
PGA	Peak Ground Acceleration

PGV	Peak Ground Velocity
PGD	Peak Ground Displacement
ASCE	American Society of Civil Engineers

## LIST OF SYMBOLS

$\varepsilon$	Strain
$f'_c$	Concrete Compressive strength
$f_y$	Steel tensile strength
$g$	Acceleration of Gravity
$I$	Building Importance Factor
$K_e$	Effective Lateral Stiffness
$K_i$	Elastic Lateral Stiffness
$M_1$	Effective modal mass for the fundamental vibration mode
$m_j$	Lumped mass at the $j^{\text{th}}$ floor level
$N$	Number of floors
$P$	Lateral Load
$R$	Ratio of elastic strength demand
$R_a$	Specific seismic load reduction factor
$R_y$	Yield strength reduction factor.
$S(T)$	Spectrum Coefficient
$S_a$	Response spectrum acceleration at the effective fundamental period
$S_d$	Response spectrum displacement at the effective fundamental period
$SD$	Standard Deviations
$T_1$	Fundamental mode period of structure
$T_0$	Characteristic period of the response spectrum

$T_e$	Effective fundamental period
$T_i$	Elastic fundamental period
$T_s$	Characteristic period of the response spectrum
$V_y$	Yield Strength
$W$	Effective seismic load
$\Delta$	Displacement
$\delta_t$	Target displacement
$\Delta_{top}$	Displacement demand
$\lambda_c$	Mean Annual Frequency of Collapse
$\sigma$	Yield stress
$\phi_1$	Normalized fundamental mode shape displacement of each storey
$\mu_D$	Ductility demand
$\Gamma$	Modal participation factor

# Chapter 1

## INTRODUCTION

### 1.1 Introduction

One of the fundamental issues in performance-based earthquake engineering is determining the seismic demand and collapse capacity proportionate to earthquakes. Consequently, various methods have been proposed for assessing seismic structural performance in development of performance-based earthquake engineering. For instance, different approaches for assessing structural collapse capacity with the aim to preserve life safety differ from the simplest approach, which may be based on a simple single-degree-of-freedom (SDOF) response model, to complex nonlinear dynamic analyses done in a structural model, which is analysed for ground motion records (Villaverde 2007). The Incremental Dynamic Analysis (IDA) is an approach which is frequently followed recently (Vamvatsikos and Cornell 2002).

Sufficient amount of demand-illustrator curves derived from different intensities of ground motions are provided for high quantity of earthquakes in order to assess the operational results of buildings statistically. Average and response dispersion are available via these curves, and accordingly a demand value corresponding to a desired probability (e.g. 84%) can be obtained (probability of 84% defines a demand value for a selected ground motion such that the demand quantity is less than the specified value based on 84% probability); such an analysis would introduce hazard

curves in which the probability of increasing the annual average of demand relative to it is specified value will be shown. This method, if matured, could have considerable benefits in estimating seismic demands in performance-based engineering (Liao et al. 2007; Zareian and Krawinkler 2007; Tagawa et al. 2008).

This method needs a huge number of inelastic time history analyses, however, it is utilized by various scholars for various usages (Liao et al. 2007; Zareian and Krawinkler 2007; Tagawa et al. 2007). In addition, many approximate models have been proposed for decreasing the computational procedures. The approximate models of IDA analysis commonly include substituting the nonlinear dynamic analysis with the pushover analysis of a structural model along with the dynamic analysis of one simple method such as the SDOF method (Han and Chopra 2006; Dolšek and Fajfar 2005; Vamvatsikos and Cornell 2005a). But, if a structure's seismic response needs to be foreseen with the most exact nonlinear dynamic analysis, the functional usage of the incremental dynamic analysis will be limited mostly because of the computational procedures which are required for conducting the incremental dynamic analysis, and also because of the concept of seismic loading, which is here defined through a series of ground motion records.

During the selection of ground motion records for incremental dynamic analysis various questions arise. The first fundamental issue is that the selected series of ground motion records reflect the seismic risk of the zone and the scaling of records is "authorized" (cf. Luco and Bazzurro, 2007). When these two situation do not exist, there may exist partiality in the structural response (Luco and Bazzurro 2007; Baker and Cornell 2006). On the other hand, accurate choice of ground motion records may

decrease the partiality in structural response (Iervolino and Cornell 2005; Shome et al. 1998).

This method is utilized by various scholars for various usages (Liao et al. 2007; Zareian and Krawinkler 2007; Tagawa et al. 2008). Considering that incremental dynamic analysis and its interpretation is accompanied by many problems, therefore in this thesis some aspects of these problems are going to be revealed.

## **1.2 Methodology**

Seismic performance of four 6, 10 and 15-story reinforced concrete buildings have been evaluated under 28 ground motion records with magnitudes over 6 in Richter scale based on incremental dynamic analysis. Fourteen far-fault and 14 near-fault records are selected to perform a comprehensive assessment. The building was designed in compliance with the ACI code specification and also, for nonlinear time history analysis, ground motion was scaled according to ASCE 07-05 standard. Preliminary studies of models are carried out by using three-dimensional frame in ETABS and then for nonlinear evaluations, the computer simulation is carried out by using the OpenSees. According to the analysis results, responses including shear profile at storeys, displacement profile of storeys, inter-storey relative displacement profile, etc. are studied. Finally overall framework to interpret the seismic responses of reinforced concrete buildings is achieved.

## **1.3 Research Objectives**

In this study, analysis on seismic shear distribution and displacement profile at stories based on near and far-fault records have been done. And also tried to investigate, how inter-story relative displacement profile changed during earthquake

(as the main source of destruction) and collapse mode based on near-fault and far-fault records has been investigated.

#### **1.4 Thesis Overview**

In this thesis, fling-steps were studied by evaluation of responses to near-fault ground motions involving fling-step. The results of this study showed that in compare to far-fault records, near-fault ones involving fling-step cause more damage to the structures. The results showed that a careful and simultaneous examination of the spectrum of acceleration and velocity, both together, can help the engineers to assess the damage potential of near-field records. The variable maximum demand which a storey has from one record to the next is the most important observation from the evaluation of non-linear time history of reinforced concrete structures.

## **Chapter 2**

### **LITERATURE REVIEW**

#### **2.1 Introduction**

A structure's appropriate seismic performance needs available strength and deformation capacities of the components to be more than the earthquake imposed necessities on the structure. Due to structural behaviour during an earthquake, performance evaluation should be carried out by nonlinear time history analysis procedure and according to selected ground shakings. If encountered to nonlinear structural behaviour, displacements are more descriptive than forces to structure and more effective control is achieved if they are bounded instead of.

A shift in design approach from force-based to that of behaviour will create a new method named performance-based design; a scheme for designing to limit states. Nonlinear analysis is a way to pass over the elastic range of structure capacity. In order to assess the seismic requirements at low operational levels, e.g. life safe and collapse prevention of structure, inelastic behaviour should be taken into widespread consideration.

One of the fundamental issues in performance-based earthquake engineering is determining the seismic demand and collapse capacity proportionate to earthquakes. Consequently, various methods have been proposed for assessing seismic structural performance in development of performance-based earthquake engineering.

In the earthquake engineering, the concept of global collapse denotes the lack of ability of a structural system for bearing the gravity loads in exposing the seismic excitation. In the earthquake engineering the concept of “collapse” denotes the lack of ability of a structural system or a part of it, for bearing the gravity load-carrying capacity under the seismic excitation. Collapse can be local or global; the local collapse can for example happen when a vertical load-carrying component is not successful in compression or when shear transfer is missed between the vertical and horizontal components (for instance shear failure between a column and a flat slab). But global collapse may have several reasons. The transference of a primary local failure from each component to another one can lead to progressive or cascading collapse (Kaewkulchai and Williamson, 2003; Liu et al., 2003). Incremental collapse happens when displacement of one story is very big, and the impacts of second order (P- $\Delta$ ) completely counterbalance the shear resistance of the first order story. In each of these cases the collapse replication requires modelling of the deterioration properties of structural components exposed to cyclic loading, as well as the inclusion of P- $\Delta$  impacts.

Some buildings collapsed partially or entirely in the following earthquakes: in alparaiso, Chile in 1985 (Leiva and Wiegand 1996; Wyllie et al. 1986); Mexico City in 1985 ( Villaverde 1991; Ostersaas and Krawinkler 1988); Armenia in 1988 (Wyllie and Filson 1989); Luzon, Philippines in 1990 (Schiff 1991); Guam in 1993 (Comartin 1995); Northridge, Calif. in 1994 (Hall 1994); Kobe, Japan in 1985 (Nakashima et al. 1998; Comartin et al. 1995); Kocaeli, Turkey in 1999 (Youd et al. 2000); Chi-Chi, Taiwan in 1999 (Huang and Skokan 2002; Uzarski and Arnold 2001); and Bhuj, India in 2001 (Jain et al. 2002). A large number of these collapses

happened in old buildings which were designed with insufficient designing standards. The other collapses related to inferior designing and construction methods in most cases. However, many collapses occurred in buildings which had been designed and built according to modern seismic designing methods. For instance, by enumerating the twenty two stores tower of the Pino Suarez complex (in Mexico City), that collapsed entirely in the 1985 earthquake (Ger et al. 1993; Osteraas and Krawinkler 1988). Hence, as the fractures in welded connections of new steel buildings during the 1994 Northridge earthquake (Bertero et al. 1994) and the 1995 Hyogoken-Nanbu earthquake (Nakashima et al. 1998) show, it can be said that many of these collapses were caused by imperfection in our information about the regional seismic risk, and the structural materials' behaviour under dynamic loads, as well as the structural systems' post-elastic behaviour. The above-said collapses lead to some questions about the sufficiency of contemporary seismic provisions for hindering an entire or partial collapse. The new seismic provisions are based on a philosophy which is based on the strong column-weak beam designs, limits of story drift, and post-elastic energy dissipation for ensuring the ability of building structures to survive in great earthquakes. Actually, some scholars have raised doubts about the accuracy of this supposition; i.e. the supposition that current code provisions are enough for preventing a structure's collapse when exposed to the extreme earthquake regarded in its design. For instance, Jennings and Husid (Jennings and Husid, 1968) assert that in case recurrent excursions in a structure's inelastic domain of deformation happen in reaction to shaking of the ground, the collected perpetual deformations of the structure can render gravity forces the dominant forces and lead to the structure's collapse by lateral instability. But this impact is not well considered in the modern designing provisions. Bernal (1987) believes that code provisions lead

to the  $P-\Delta$  impact of gravity loads for an insufficient extrapolation of the outcomes of static elastic behaviour. In addition, Bernal (1992) in the investigation of the instability of buildings in earthquakes, asserts that only by limiting the structure's maximum elastic story drifts we cannot guarantee a structure's immunity against inelastic dynamic instability. This conclusion is confirmed recently by Williamson (2003). Also, Challa and Hall (1994) in their study of the collapse capacity of a twenty story steel frame, see significant plastic hinging in the columns of the structure and the structure's possible collapse when exposed to ground motions in a great earthquake. Although according to what is needed in current code provisions, the flexural strength of the columns is more than its beams in all of the joints. It is worth mentioning that this remark is recently confirmed by Medina and Krawinkler (2005).

In fact, in a research to analyse the strength demands of so many regular moment-resistant frames in various ground motions, these two researchers found out that the potential of formation of plastic hinges in the columns is high in regular frames which are designed in accordance to the strong column-weak beam needs of new code provisions. In a research similar to Challa and Hall, Martin and Villaverde (1996) also found out that a 2-story, 2-bay frame structure will collapse in a relatively strong ground motion even in cases that the structure observes all the needs of the 1992 AISC seismic provisions (AISC 1992). Similarly, in a research carried out with an eight-story steel frame, Roeder et al. (1993) and Schneider (1993) realized that the minimum designing criteria needed by the 1988 Uniform Building Code [International Conference of Building Officials (ICBO), 1988] are not sufficient to guarantee that the structure's inelastic story drifts are constantly below

the maximum numbers considered in its designing. Therefore, modern structures' collapse in the past earthquakes and the unsubstantiated sufficiency of the current designing standards for hindering such collapses arise the question that what is the real safety margin of the structures facing a collapse as a result of earthquakes. This question again has gained importance because of the profession's desire for moving toward performance based designing. We know that preventing from the collapse is an aims of the performance-based design, and also one of its commitments is to ensure an acceptable safety margin against collapse in the maximum seismic load expected. But at the present time, as various researchers have indicated (AstanehAsl et al. 1998; Hamburger 1997; Bernal 1998; Esteva 2002; Griffith et al. 2002; Li and Jirsa 1998), there isn't any firmly settled method (except the cooperative opinion of the code writers) to estimate this safety margin. Furthermore, it is not clear whether the analytical tools available are sufficient for analysing it in a trustworthy way because the collapse process includes huge deformations, considerable second order effects, as well as a complicated degradation of material as a result of the localized events like cracks, local buckling, and also yielding. The more unfavourable point is that apparently there are even no acceptable criteria for identifying when and how a collapse of structures occurs as a result of the effect of dynamic loads. That is because it is not enough to reach an unstable condition (for instance a single and useful stiffness matrix) for inferring a structure's collapse under the dynamic loads because unloading immediately after the structure obtains this unsteady condition can regain its steadiness (Araki and Hjelmstad 2000).

## **2.2 Previous Research on Global Collapse**

Several aspects of collapse assessment methods are improved nowadays. Scholars have tried independently to understand and quantify the P- $\Delta$  effects and to develop

nonlinear deteriorating component models which could duplicate the experimental results. Besides, efforts have been done for integrating the factors that affect the collapse in an integrated methodology.

### **2.2.1 P- $\Delta$ effects**

The investigation of the global collapse initiated by P- $\Delta$  effects in seismic reaction. However, hysteretic models took a positive post-yielding stiffness into account the structure tangent stiffness turned negative in huge P- $\Delta$  effects that finally led to the system's collapse. For example, Jennings and Husid (1968) used a one story frame which had springs at the ends of the columns by the use of bilinear and hysteretic models. They inferred that the most significant factor in collapses is the structure's height, the ratio of the earthquake intensity to level of the yield of the structure, and the second slope of the bilinear and hysteretic model. They asserted that the required motion intensity for collapse depended firmly on ground motion duration. This conclusion was drawn without consideration of cyclic deterioration behaviour, and simply because the likelihood of collapse increases when the loading path stays for a longer time on a backbone curve with a negative slope.

Sun et al. (1973) investigated the impact of gravity on the dynamic behaviour of the SDOF system and its impact on changing the system's period. Bernal (1992, 1998) analysed two-dimensional moment-resisting frames, and inferred that the least required strength (or base shear capacity) for enduring a ground motion without collapse absolutely depends on the form of the controlling mechanism.

### **2.2.2 Degrading Hysteretic Models**

In the degrading hysteretic model, degradation of the reloading stiffness depends on maximum displacement occurred in the loading path direction. As a result of this attribute, this model is frequently called the peak-oriented model.

In 1970, Takeda (Takeda, 1970) proposed a model with a tri-linear backbone which degraded the unloading stiffness on the basis of the system's maximum displacement. This model was designed for the reinforced concrete components (RC), in which the envelope is tri-linear due to the fact that it involves a part for the uncracked concrete. Besides the models which had piecewise linear behaviour, some smooth hysteretic models are proposed that involve a constant stiffness change because of the changes in yielding and sharp as a result of the unloading, which is the Wen-Bouc model (Wen, 1976).

Song and Pincheira's model (2000) can also represent the stiffness deterioration and cyclic strength on the basis of dissipated hysteretic energy. This model is basically a peak oriented model which regards the pinching on the basis of deterioration factors. The backbone curve contains a kind of post capping negative stiffness as well as a branch of residual strength. Due to the fact that the original backbone curve doesn't deteriorate, the unloading and accelerated cyclic deterioration are the mere modes, and before arriving to the peak strength, the model is not able to reproduce the strength deterioration.

Ibarra et al (2005) developed a tri-linear model similar to that of Song and Pincheira (2000) which was able to take strength deterioration in to account completely. Based on the results of 320 tests performed on columns around the world, relations are

presented for seismic behavioural parameters of the beam-column elements. In order to study structural behaviour and determination of instabilities, Haselton et al (2007) utilized linear regression analysis on PEER dataset (collected at Washington university by Berry and Eberhard, 2003 including unilateral and reciprocating tests on 306 rectangular and 177 circular beam-columns) to calibrate the data presented by Fardis and Panagiotakos, 2003 and Ibarra et al, 2005. Finally some relations were derived for the necessary parameters to introduce monotonic and cyclic behaviour herein.

These relations were somewhat suitable for modelling the elements of regulatory-designed buildings. The model utilized by Haselton et al (2007) can be applied to consider the nonlinear behaviour of beam-column elements of trilinear model offered by Ibarra et al (2005). This model was implemented in OpenSees by Al.Toontash (2004).

One important attribute of this model is to have a negative branch after the hardening region which enables us to model strain softening appears in phenomenon like concrete crushing or buckling and failure of armatures.

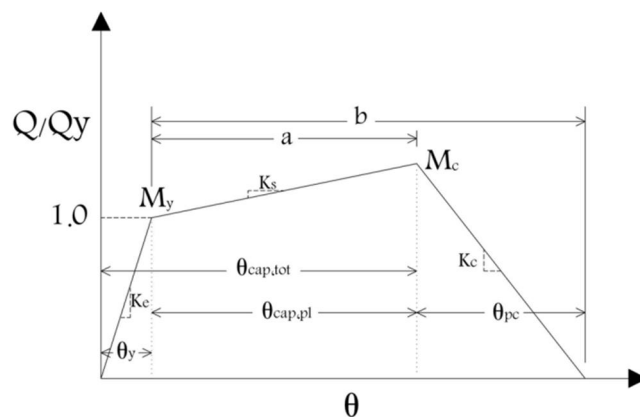


Figure 2.1. Model offered by Ibarra (2005)

### 2.2.3 Analytical Collapse Investigations

Takizawa and Jennings (1980) studied the final capacity of an RC frame in seismic excitations. This structural model was an equivalent SDOF system which involved degrading tri-linear and quadric-linear (or strength degrading) hysteretic curves. This is a primary effort to evaluate P- $\Delta$  effects as well as material deterioration in collapse evaluation. They used some modified Takeda models to indicate that the SDOF systems which had negative post-yield stiffness tend to collapse, either if they had experienced the damage before or not.

Mehanny and Deierlein (2000) examined collapse for some composite structures which had RC columns as well as the steel or composite beams. For a structure and ground motion (GM) intensity record, these researchers performed a second-order inelastic time history analysis (THA) for the undamaged structures and computed the cumulative damage indices, which were used to degrade stiffness and strength of the damaged sections. They reanalysed the damaged structure via a second-order inelastic static analysis with respect to the residual displacements and involving just gravity loads. It was supposed that the Global collapse occurs in case the maximum vertical load that the damaged structure is able to endure is less than the applied gravity loads ( $\lambda_u < 1$ ). In case the collapse did not occur, then the record would be scaled to determine the ground motion intensity in which the collapse happens.

Lee and Foutch (2001) analysed the performance of new moment-resisting steel frames in the FEMA/SAC project. These analytical models involved a fracturing element used by Shi (1997) in Drain-2DX program. In order to analyse the global drift capacity in the SAC buildings, these researchers made use of the “IDA” approach (Vamvatsikos and Cornell, 2002). The beginning of the global dynamic

instability was explained as the spot where the IDA curve local slope reduced to less than 20% of the first slope of IDA curve in the elastic region. The frames were exposed to sets of 20 SACGMs. Similarly, Jalayer (2003) employed the IDA concept in order to estimate the global dynamic instability capacity of a regular RC structure. Jalayer included strength deterioration resulted from shear failure of the columns on the basis of the model proposed by Pincheira et al. (1999).

Williamson (2003) investigated the response of some SDOF systems which were exposed to various ground motion records like P- $\Delta$  effects and material deterioration on the basis of a modified form of the damage model of Park and Ang (2003). He discovered great sensitivity to the characteristics of the structure as well as the ground motion characterization.

Adam and Krawinkler (2003) studied the distinction in the greatly nonlinear systems response in various analytical formulations. They inferred that huge displacements formulation creates nearly the exact responses as conventional (or small displacement) formulations do, even when the collapse is close.

#### **2.2.4 Evaluating the Expected Spectral Shape Effect on Collapse Assessment**

Another challenge in assessing structural collapse capacity by nonlinear dynamic analysis occurs in case of ground motions selection and scaling for the analysis. Baker and Cornell (2005) indicated that the spectral shape, along with the ground motion intensity, is an important trait of ground motions which has an influence on the structural response. Especially, for a certain level of ground-motion hazard (for instance a 2 percent chance of exceedance in 50 years), the form of the Uniform Hazard Spectrum (UHS) may be totally different from the form of the mean or the

anticipated response spectrum of an actual ground motion which has a similarly high spectral magnitude in one period (Baker and Cornell 2006; Baker 2005).

$\varepsilon$  (i.e., epsilon) can be defined as the number of logarithmic standard deviations among the spectral value and the mean  $S_a$  prediction in a ground-motion prediction or “attenuation” model.

In order to show the unique spectral form of some rare ground motions, the Loma Prieta spectrum (1989) includes a rare spectral intensity at 1.0 s of 0.9 g, which involves only a 2 percent chance of exceedance in 50 years. It is revealed that this extreme ground motion has a very different form than the mean anticipated spectrum. Especially, the spectrum of this record has a peak from nearly 0.6 to 1.8 s and lesser intensities in proportion to the predicted spectrum in other times. The intensity at 1.0 s, excelled with a 2 percent probability in 50 years, exists in the peak of the spectrum, and in this time the observed  $S_a(1\text{ s})=0.9\text{ g}$  is very higher than the mean expected  $S_a(1\text{ s})=0.3\text{ g}$ ; in other points far from the peak, the spectral values are more similar to the mean expected  $S_a$ . This peaked shaped exists because the ground motions, which have an intensity above the average, do not always have equal and large intensities in other points.

In a 1.0 s period, the spectral value of the Loma Prieta record is 1.9 standard deviations higher than the anticipated mean spectral value from the attenuation connection, hence this record will have “ $\varepsilon=1.9$  at 1.0 s.”  $\varepsilon$  (or epsilon) is defined as the number of logarithmic standard deviations between the spectral value observed and the mean  $S_a$  prediction from a ground-motion prediction or attenuation model. Correspondingly, this record has  $\varepsilon=1.1$  in 1.8 s. Hence, the component  $\varepsilon$  is a function

of the ground-motion record, the ground-motion prediction model which is compared, and the desirable period.

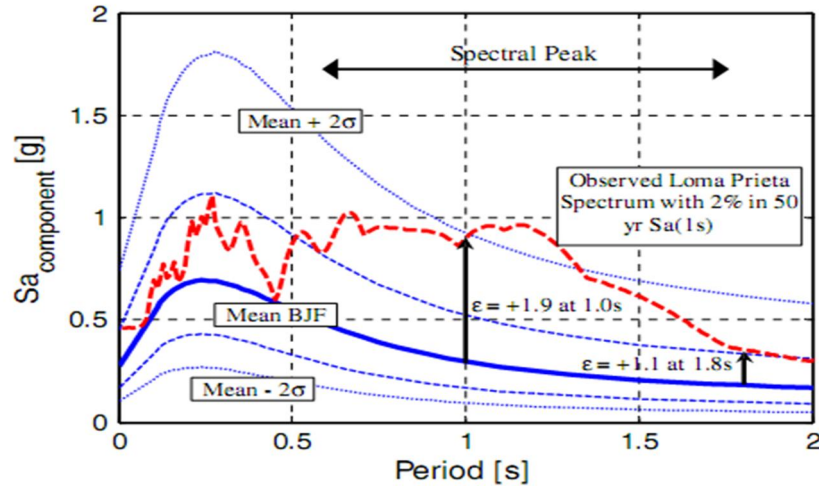


Figure 2.2. Comparison of an observed spectrum from a Loma Prieta motion with spectra predicted by Boore et al. (1997); after Haselton and Baker (2006)

Baker and Cornell (2005) investigated the effects of several ground-motion characteristics on the collapse capacity of a no ductile reinforced concrete (RC) frame 7-story building with an important period  $T_1$  of 0.8 s. They discovered that the average collapse capacity raised by a factor of 1.7 when a  $\varepsilon(0.8s) = 2.0$ .

### 2.2.5 Experimental Collapse Investigations

A large number of experiments have been performed to relate collapse with shear failure and ultimately with axial failure in the columns. For instance, Yoshimura and Yamanaka (2000) tested some reinforced concrete columns subjected to low axial load. They detected that lateral and axial deformation and the input energy in the collapse are different according to the loading protocol which is imposed on each specimen. From the other point of view, the ratio of the vertical deformation increment to lateral deformation increment in collapse does not differ with the loading path. They inferred that collapse happens when the lateral load is reduced to

about 10 percent of the maximum load. Yoshimura (2002) evaluated columns experiencing shear failure before the flexural yielding and others failing in shear after the flexural yielding. They concluded that axial failure happens when the shear capacity decreases to nearly zero.

Sezen (2002) tested building columns of full scale shear-critical reinforced concrete under the cyclic lateral loads up to the point where the column can no longer bear the axial load. These tests revealed that the loss of axial load doesn't always come just after loss of the lateral load capacity. Elwood and Moehle (2002) believed that shear failure in columns doesn't always result in the collapse of the system. Shear failure usually is accompanied by a reduction of axial capacity that depends on several factors. They discovered that in columns with lower axial loads, the axial load failure happens in somewhat large drifts, without considering if the shear failure occurred immediately or whether the shear failure occurred in very smaller drift ratios. In case of the columns with bigger axial loads, the axial load failure usually occurs in smaller drift ratios, and may occur right after the loss of lateral load capacity. Additionally, they gathered data to develop an empirical model for estimating the shear strength deterioration.

Vian and Bruneau (2001) performed some shake table experiments of a SDOF steel frame system exposed to earthquakes of gradually increasing intensity until the collapse as a result of the geometric nonlinearities (P- $\Delta$  effect). They inferred that the stability coefficient involves the most important impact on the structure's behaviour. By the increase in this coefficient, the maximum sustainable drift and spectral acceleration which can be inhibited before the collapse will be decreased. Kanvinde

(2003) extended the work of Vian and Bruneau (2001) by testing additional SDOF systems. He discovered that the current methods of nonlinear dynamic analysis like the Open Sees platform (OpenSees, 2002) are extremely precise for predicting the collapse for systems in which the P- $\Delta$  effect controls the beginning of collapse.

Finally, despite the large amount of researches and studies on this topic, the response of structural systems under geometric nonlinearities and material deterioration has not been studied in details. Hence, there is a need for conducting systematic research about the global collapse with respect to all sources that result in this limit situation.

### **2.3 Description of Global Collapse Assessment Approach**

Generally speaking, global collapse refers to the lack of ability of a system to support gravity loads due to the extreme lateral displacement, which significantly reduces the story shear resistance and produces instability in the system. Traditionally, collapse potential was estimated by using non-deteriorating systems in order to predict the engineering demand parameters (EDPs) and assigning judgment limits for these parameters. Recently, the deteriorating systems have been used for estimation of collapse but still based on pre-established EDPs limits. However, EDPs become very sensitive when the system is very near to collapse, and small disturbance of the input creates great variations in the response. Hence, in the proposed methodology global collapse is described by a relative intensity measure instead of an EDP. The relative intensity measure is defined as the proportional relation of the ground motion intensity to a structural strength parameter. In the present research, the ground motion intensity measure is the spectral acceleration in the fundamental period of the structure normalized by the acceleration of gravity ( $g$ ), and the strength parameter is the yield strength of the structure which is normalized by its seismic weight. For a

certain structure and ground motion, the collapse evaluation consists of a series of dynamic analysis starting with a relative intensity that produces an elastic response for the system. Then the relative intensity is increased until collapse takes place. The relative intensity at collapse is called the collapse capacity.

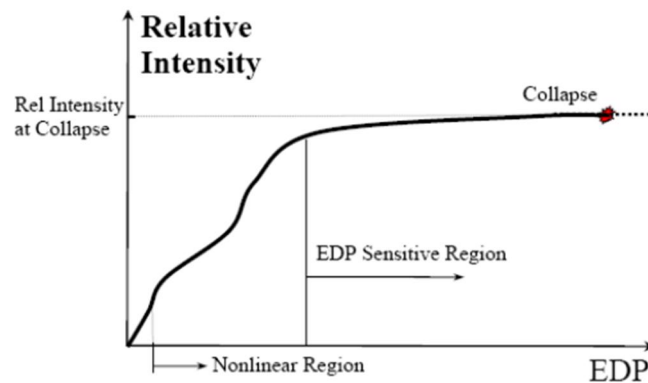


Figure 2.3. EDP curve, relative intensity (Vamvatsikos and Cornell, 2002)

This process requires the analytical reproduction of collapse and the modelling of deterioration properties of structural elements. The use of deteriorating models allows the redistribution of damage and considers the capability of the system to maintain significantly larger deformations than those related to reaching the ductility capacity in one element.

### 2.3.1 Selection of Ground Motions

The global collapse method is based on the time history analysis. Therefore, a set of ground motions should be selected cautiously based on the specific goals. The set must be large enough to produce statistically reliable results.

### 2.3.2 Deterioration Models

Collapse evaluation is based on hysteretic models that account for history-dependent strength and stiffness deterioration. Deteriorating models are developed for bilinear, peak-oriented, as well as pinching hysteretic models. These systems' monotonic

backbone curve includes a negative tangent stiffness branch, an elastic branch, a strain-hardening branch, and in some cases a residual strength branch of zero slope. In addition, cyclic deterioration is considered by making use of energy dissipation as a deterioration criterion. The following 4 modes of deterioration are involved: post-capping strength, basic strength, accelerated reloading stiffness deterioration, and unloading stiffness. It is shown the response of an SDOF system represented by a peak-oriented model with rapid cyclic deterioration.

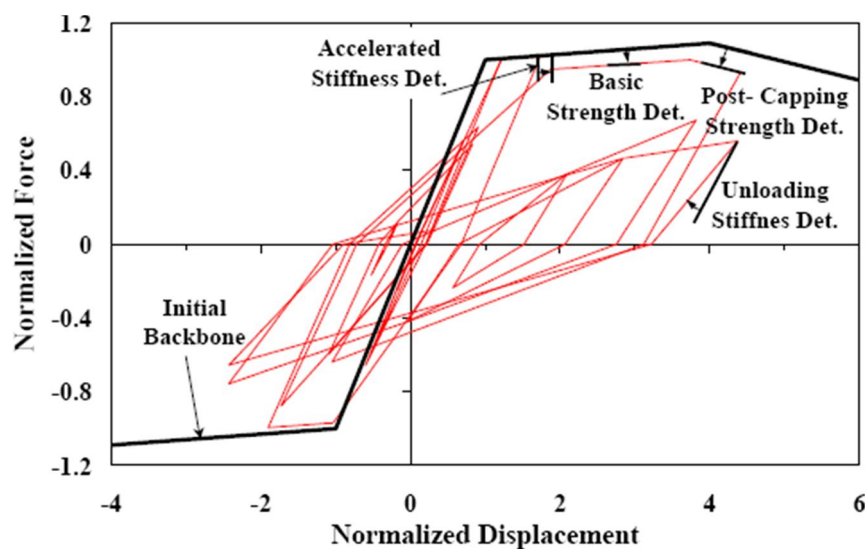


Figure 2.4. The response of an SDOF system represented by a peak-oriented model with rapid cyclic deterioration (Luis F. Ibarra and H. Krawinkler, 2004)

### 2.3.3 Structural Systems

In general, the collapse assessment methodology is identical for SDOF and MDOF systems. A variety of SDOF systems are used in Chapter 4 to determine the parameters that most affect global collapse. The information synthesized from SDOF systems is used to narrow the number of parameters to be studied in MDOF structures.

### 2.3.4 Collapse Capacity

To obtain the collapse capacity related to a particular ground motion, the structural system is analysed under increasing relative intensity values, expressed as  $(S_a/g)/\eta$  for SDOF systems. The intensity of the ground motion ( $S_a$ ) is the 5% damped spectral acceleration in the elastic period of the SDOF system (without P- $\Delta$  effects), while  $\eta = F_y/W$  is the base shear strength of the SDOF system which is normalized by its seismic weight. The relative intensity can be plotted against the *EDP* of interest, resulting in  $(S_a/g)/\eta$ - *EDP* curves.

For MDOF structures, the relative intensity is expressed as  $[S_a(T_1)/g]/\gamma$ , where  $S_a(T_1)/g$  is the normalized spectral acceleration in the structure's fundamental period without P- $\Delta$  effects, and the parameter  $\gamma$  is the base shear coefficient  $V_y/W$ , which is equivalent to  $\eta$ . These relative intensity definitions permit a dual interpretation:

(1) If there be an increase in the ground motion intensity and the system strength is kept constant, the resulting  $(S_a/g)/\eta$  - *EDP* or  $[S_a(T_1)/g]/\gamma$  - *EDP* curves represent incremental dynamic analyses (IDAs) (Vamvatsikos and Cornell, 2002).

(2) In case the ground motion intensity is kept constant (given hazard) and the strength of the system is reduced, the resulting  $(S_a/g)/\eta$  - *EDP* or  $[S_a(T_1)/g]/\gamma$  - *EDP* curves represent *EDP* demands for various strength levels and are referred to as "strength variation curves." In this case,  $(S_a/g)/\eta$  is equal to the conventional strength reduction factor,  $R$ , for structures without over strength. Note that when the strength is decreased the entire backbone curve scales down.

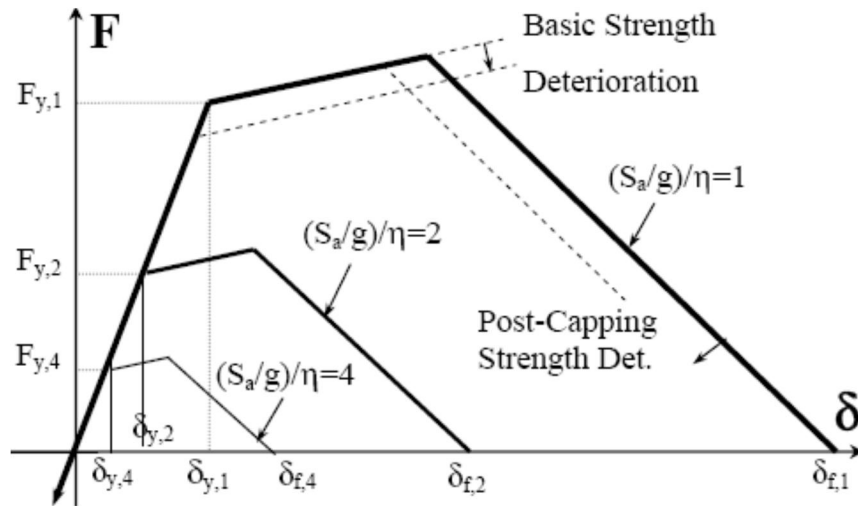


Figure 2.5. Different pushover curves for  $(S_a/g)/\eta$  (Ibarra and Krawinkler, 2005)

### 2.3.5 Effects of Uncertainty in System Parameters

In the first part of the research, the collapse capacity is examined considering record to record variability (RTR) as the only uncertainty in the computation of the collapse capacity. However, system parameters like ductility capacity and post-capping stiffness can also be considered in a probabilistic framework, even though experimental information that can be used to define statistical properties of the parameters of the hysteresis model is rather limited.

The first-order second-moment (FOSM) method is utilized for computation of the additional variance of collapse capacity resulting from the uncertainty in the system parameters, while Monte Carlo simulation is also utilized in order to verify some of the results. The FOSM method approximates the collapse capacity variance based on a Taylor's series expansion of a performance function ( $g$ ) about the anticipated values of random variables. One of the main advantages of the method is that the first and second moments are appraised without any knowledge about distribution of the function " $g$ ." For instance, it is indicated that the contributions to the variance of

collapse capacity from several sources, including RTR variability, ductility capacity, uncertainty in post-capping stiffness, and cyclic deterioration, considering a standard deviation of the log of the data of 0.60.

The example does not include correlation among the different parameters. Based on the system properties, the contributions of uncertainty in system parameters to the total variance can be small or comparable to the contribution due to RTR variability.

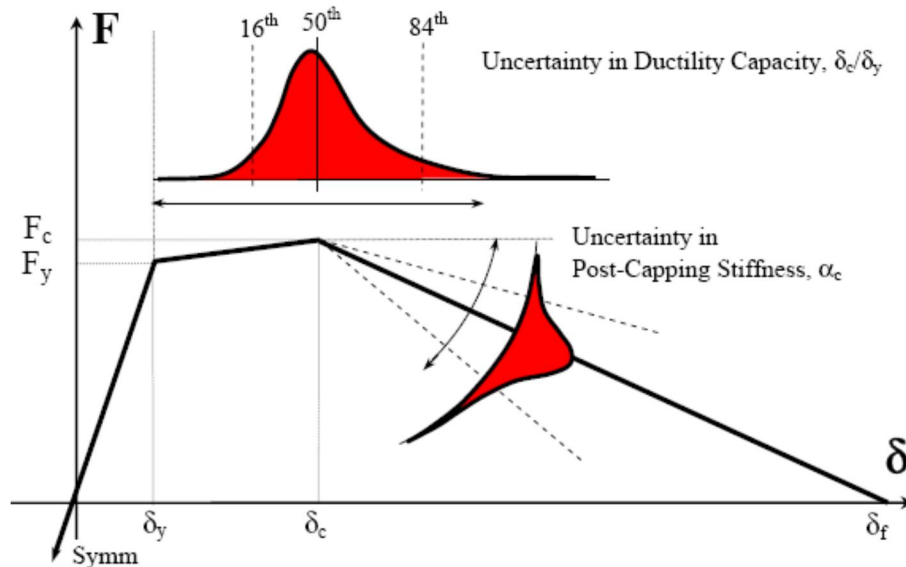


Figure 2.6. Uncertainty in system parameters (Vamvatsikos, 2002)

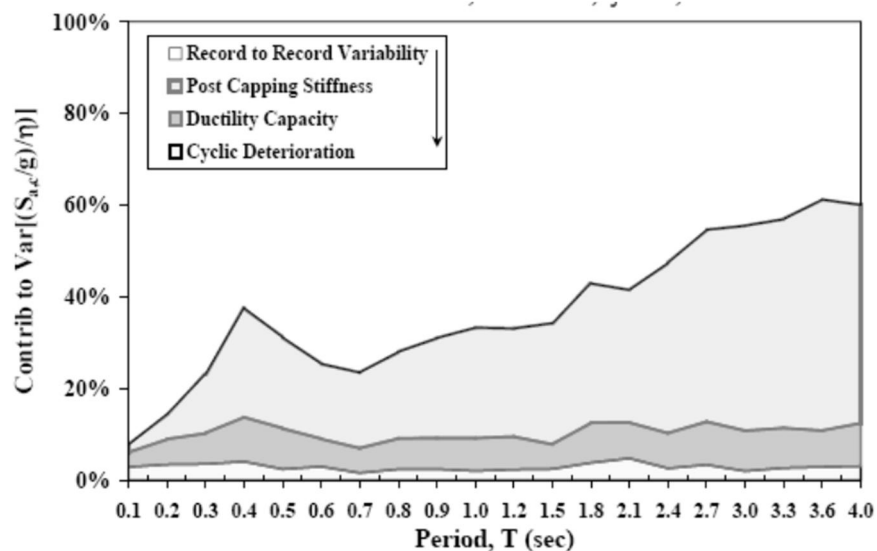


Figure 2.7. Effect of uncertainties on system parameters with different (Song, 2002)

## **2.4 Collapse Assessment of SDOF Systems**

Parameter studies on SDOF systems are easily implemented and help to identify the system parameters which can have an insignificant or prominent influence on MDOF structures. The small calculation effort required for analyzing the SDOF systems allows the investigation of so many systems. Furthermore, modification of a special parameter usually has a larger impact on SDOF systems than on MDOF structures. The latter structures usually have elements yielding in various times and some of the factors do not reach the inelastic range; thus, their global stiffness matrix has smaller modifications than the corresponding stiffness of SDOF systems.

In the past, many studies have been conducted to evaluate the inelastic seismic demands of SDOF systems. Seismic demands have been studied by means of constant ductility inelastic displacement ratios (Miranda, 1993, 2000) or by means of strength reduction factors for constant ductility (Nassar and Krawinkler, 1991; Rahnema and Krawinkler, 1993). The second study included the effect of strength and stiffness deterioration in hysteretic models with bilinear backbone curves. The results indicated that strength deterioration may greatly affect the response of SDOF systems, but the effects of unloading stiffness deterioration are relatively small. Gupta and Kunnath (1998) extended the investigation of Rahnema and Krawinkler (1993), obtaining similar conclusions. However, these studies are based on systems without strength deterioration of the backbone curve and they do not address the collapse limit state. Song and Pincheira (2000) investigated the impact of stiffness and strength deterioration on the SDOF systems maximum inelastic displacement without including geometric nonlinearities. They discovered that the displacement proportion between a deteriorating and non-deteriorating system can be about two

(particularly in the short-period range) and that it differs meaningfully with the deterioration rate and type of ground motion. They assumed that an SDOF system collapses if its remaining strength is less than 10% of the yield strength. They reported that many systems collapsed for one or more ground motions under low strength coefficients but they did not trace this limit state for all the cases. Vamvatsikos (2002) performed the incremental dynamic analyses (IDAs) for pinched hysteretic SDOF systems which involved a negative post-capping stiffness and residual strength although without any cyclic deterioration. He detected that the cap displacement ( $\delta_c$ ) and the slope of the post-capping stiffness constitute the two factors that have the greatest influence on the performance of the medium-period-systems. Ibarra and Krawinkler (2005) investigations aimed to have an innovation for global collapse assessment of deterioration-oriented structural systems.

## Chapter 3

### INCREMENTAL DYNAMIC ANALYSIS

#### 3.1 Introduction

The Incremental dynamic analysis has lately appeared as an influential tool for investigating the general behaviour of structures, from their elastic response via yielding and nonlinear response to global dynamic instability (FEMA 2000a). An incremental dynamic analysis includes conducting several nonlinear dynamic analyses during which the intensity of the ground motion chosen for collapse evaluation is incrementally increased so as to reach the structure's global collapse capacity. In addition it includes designing a measure of the ground motion intensity (such as the spectral acceleration in the structure's basic natural period) against a response parameter (demand measure) like peak story drift ratio. The global collapse capacity is reached at the time that the curve becomes flat in this plot. It means when a little increase in the ground motion intensity produces a huge increase in the structural response. Due to the fact that various ground motions (like ground motions with various frequencies content and various durations) result in different intensity versus response plots, this analysis is done again under various ground motions in order to achieve significant statistical averages.

Incremental dynamic analyses were developed primarily in 1977 (Bertero 1980) and have been recently investigated comprehensively by different researchers. For

instance, Vamvatsikos and Cornell (2002) described this method thoroughly, determined the intensity-response curves for various structures, examined the characteristics of the response-intensity curves, and proposed some techniques for performing an incremental dynamic analysis effectively and summarized the final results of various curves produced by several ground motions. These scholars observed that the incremental dynamic analyses are the useful means that address the seismic demands on structures and their global capacities simultaneously. In addition, they asked for the attention toward abnormal characteristics of the response-intensity curves like collapse capacities, no monotonic behaviour, discontinuities, multiple and their extreme variability from each ground motion to the other one. Vamvatsikos and Cornell (2004) recognized that a thorough incremental dynamic analysis needs an accurate computational endeavour, proposed a functional method for performing it effectively, and then by means of a specific example of a 9-storey moment-resisting steel frame they indicated how to apply it, how to explain the findings, and how to utilize the results in performance-based earthquake engineering. Also, Vamvatsikos and Cornell (2005), through revealing the connection between an incremental dynamic analysis and a static pushover analysis, developed a simple method for estimating the collapse capacities and seismic demands of multi degree of freedom structures by means of an equivalent single degree of freedom system.

Similarly, Ibarra and Krawinkler (2004) developed a methodology for evaluating the global collapse capacity of deteriorating frame structures in earthquake ground motions. This methodology was based on the utilization of a relative intensity measure, defined as  $S_a(T_1) / g / \gamma$ , in which  $S_a(T_1)$  represents the 5 percent damping

spectral acceleration in  $T_1$ , the structure's basic period; also  $g$  is the acceleration resulting from gravity; and  $\gamma$  is a shear coefficient which is equal to  $V_y / W$ , in which  $V_y$ =yield base shear without P- $\Delta$  impacts and  $W$ =weight of the structure. In case of the structures without over-strength, this intensity measure equals to the reduction factor which is used in building codes for analysing the yielding structures. Furthermore, this methodology is based on the utilization of deteriorating hysteretic models for representing the structural components' cyclic behaviour during intensive inelastic deformations. These deteriorating models create the significant modes of deterioration which are observed in the experiments. In order to investigate the collapse capacity, these scholars increases the intensity measure up to the point that the intensity measure vs. normalized maximum roof drift curve turns to a flat shape. This relative intensity in which the curve assumes a flat shape is subsequently regarded as the structure's collapse capacity. By making use of a probabilistic format for considering uncertainties in the frequency of ground motions and the deterioration properties of the structural elements, the evaluation is performed. Ibarra and Krawinkler (2004) subsequent to the implementation of the deteriorating hysteretic models in a computer program called Drain- 2DX (Prakash et al. 1993), made use of this developed methodology in order to first, conduct a parametric investigation with particular frame structures and examine the impact of various factors on the structures' collapse capacity; second, indicate collapse fragility curves, and third, determine the mean annual frequency curves. The structures used in the parametric investigation are stiff and flexible single-bay frames which had 3, 6, 9, 12, 15, and 18 stories with their plasticity focused at the beam ends and the columns' base; it means that the plastic hinges are just allowed to be formed in the beam ends and in the columns' base. In the parametric investigation viewpoint, they discover

that the main two factors that have a great impact on the collapse of a structure are the slope of post-yield softening branch in the moment rotation relation of the yielding members and the displacement in which this softening starts. They also found out that the cyclic deterioration (and consequently the ground motion duration) is an essential but not a dominant factor in structures' collapse. This finding opposes with the results obtained by Takizawa and Jennings (1980) who inferred that collapse is to a great extent affected by the ground motion duration.

In a parallel research, Ayoub et al. (2004) studied the impact of stiffness and strength degradation on the structures' seismic collapse capacity. In order to meet this aim, they conducted an incremental dynamic analysis of a single degree of freedom structure with a normal period of 1.0 s and they considered three degrading fundamental models that clearly explain the collapse possibility. They also plotted collapse fragility curves for this system. The fundamental models considered strength softening (the negative stiffness branch) and strength and stiffness degradation under cyclic loading. It is supposed that collapse happens when the system's strength is decreased to zero. The three considered fundamental models include: 1) bilinear model, 2) modified Clough model, and 3) pinching model. An energy-based criterion is utilized for defining the strength softening and stiffness as well as the strength degradation. The study is conducted through utilizing a group of 80 ground motions and various degradation levels. They discovered that for certain ground motion intensity the possibility of systems collapse with low degradation is like the systems with average degradation. On the contrary, this possibility is really higher in case of systems with high degradation. Ibarra et al. (2005) observed that collapse evaluation needs hysteretic models which are able to reproduce all of the significant modes of

deterioration recognized in the experiments and they similarly studied the influence of stiffness and strength degradation on the seismic demands of structures as they go near to collapse. Consequently, they proposed some simple hysteretic models that include stiffness and strength deterioration characteristics; calibrated them by means of experimental information from steel, plywood, and reinforced concrete components tests; and then determined employing instead some of the developed models the response of a single degree of freedom system with a normal period of 0.9 s and a damping ratio of 5 percent under a group of 40 ground motions. They also scaled these ground motions to different intensity levels and developed demand versus intensity curves in order to investigate the system collapse capacity in each case. They inferred that deterioration is a crucial consideration in seismic response analysis of a structure when it is close to collapse limit state.

Eventually, Lee and Foutch (2002) studied the performance of 20 steel frame buildings designed on the basis of the 1997 NEHRP provisions recommendations (FEMA 1998) and considering prequalified post-Northridge beam-column relations. For this reason, the buildings are exposed to a nonlinear time-history analysis in a group of 20 earthquake ground motions. They scaled the ground motions for a performance objective of preventing the collapse, in order to have spectral accelerations with a 2 percent possibility of exceeding in 50 years. The analytical models utilized in the analysis, are responsible for ductility of the beam column joints, the panel zone deformations, and the effect of interior gravity frames. The behaviour of the beam-column joints is described by progressive strength degradation after a 0.03 rad rotation. They compared the maximum story drift demands against the buildings' drift capacities in order to evaluate the buildings'

performance for the collapse prevention objective. Local and global drift capacities are taken into account in this comparison. The local drift capacities are the most drift angle that the beam column joints can maintain before losing their gravity load carrying ability. According to the findings of the full-scale experiments, they considered a 0.07 rad local drift capacity. The global drift capacities are decided by conducting the incremental dynamic analysis for each building and developing the related maximum story drift ratio versus spectral acceleration curves. The global drift capacity of a building is regarded the maximum story drift ratio in which the maximum story drift ratio versus spectral acceleration curve turns into a flat shape, or, instead, the maximum story drift ratio in which this curve reaches a slope which is equal to 20% of the slope in the elastic region of the curve. On the other hand, if this slope is not acquired before a story drift ratio of 0.10 is attained; it is supposed that the global drift capacity is equal to 0.10. Lee and Foutch (2002), according to the computed drift demands and the supposed local and global capacities, inferred that all buildings in the study meet the objective of collapse prevention.

## **3.2 Fundamentals of Incremental Dynamic Analysis**

### **3.2.1 Introduction**

Incremental Dynamic Analysis (IDA) is a kind of parametric analysis that appeared in various forms in order to estimate the structural performance under seismic loads more thoroughly. It includes exposing a structural model to one (or several) ground motion records, each of which is scaled to different levels of intensity, and hence creating one (or more) curves of response parameterized versus intensity level. In order to establish a common frame of reference, the fundamental concepts are examined, an integrated vocabulary is presented, acceptable algorithms are proposed,

and the characteristics of the IDA curve are examined for single degree of freedom (SDOF) and multi-degree of freedom (MDOF) structures.

The development in computer processing has led to a continuous drive towards the more accurate but more complex methods of analysis. Therefore, the state of the art has gradually moved from elastic static analysis to dynamic elastic, nonlinear static and eventually the nonlinear dynamic analysis.

This idea was proposed early in 1977 by Bertero (1977), and has been used in various forms by many researchers including, Yun et al. (2002), Luco and Cornell (1998, 2000), Bazzurro and Cornell (1994a, b), Nassar and Krawinkler (1991, pg.62–155) Dubina et al. (2000), De Matteis et al. (2000), and Psycharis et al. (2000). In recent years, it has also been used by the U.S. Federal Emergency Management Agency (FEMA) guidelines (FEMA, 2000a, b) as the Incremental Dynamic Analysis (IDA) and accepted as the state of the art method to determine the global collapse capacity. The study of IDA is nowadays a multipurpose and beneficial method and some of its goals include:

- Complete recognition of the response range or demands versus the potential level range of a ground motion record.
- Superior understanding of the structural implications of rarer or more severe levels of ground motion.
- Superior understanding of the alterations in the nature of structural response by the increase in ground motion intensity (like changes in peak deformation patterns with height, start of stiffness and strength degradation as well as their magnitudes and patterns).
- Providing estimations of the global structural system dynamic capacity.

- Ultimately, in a certain multi-record IDA study, the stability rate (or variability) of all these elements from a ground motion record to another.

### 3.2.2 Fundamentals of Single-Record IDAs

First of all, every required term should be clearly defined, and then we will start developing our methodology by means of scaling an acceleration time history as a basic block.

Suppose that we have an acceleration time-history, chosen from a ground motion database, which will be called the base, as-recorded (though it may be pre-processed by seismologists, such as baseline corrected, rotated and filtered), unscaled accelerogram  $a_1$ , a vector with elements  $\vec{a}_1(t_i), t_i = 0, t_1, \dots, t_{N-1}$ . In order to take more severe or milder ground motions into account, a simple transformation will be presented by uniformly scaling the amplitudes up or down via a scalar  $\lambda \in [0; +\infty)$ :  $\lambda \vec{a}_1 = \vec{a}_\lambda$ .

Definition 1: The Scale Factor (SF) of a scaled accelerogram,  $\vec{a}_\lambda$  is the non-negative scalar  $\lambda \in [0; +\infty)$  that creates  $\vec{a}_\lambda$  when it is multiplicatively applied to the unscaled (natural) acceleration time-history.

Although the SF is the simplest way for characterization of the scaled pictures of an accelerogram, it is not easy for engineering purposes because it provides no information of the actual power of the scaled record and its impact on a certain structure. A more functional item may be a measure that would map to the SF one to one, but still it would be more informative, for better relating to its damaging potential.

Definition 2: A Monotonic Scalable Ground Motion Intensity Measure (or intensity measure, IM) of a scaled accelerogram,  $\vec{a}_\lambda$  is a non-negative scalar  $IM \in [0; +\infty)$  which makes a function,  $IM = f_{\vec{a}_1}(\lambda)$ , that is dependent on the unscaled accelerogram,  $\vec{a}_1$  and is increasing monotonically with the scale factor,  $\lambda$ .

Although there are many proposed quantities for characterizing the intensity of a ground motion record, it might not be constantly clear how to scale them, for example Moment Magnitude, Duration, or Modified Mercalli Intensity; these must be marked as non-scalable. Some usual instances of scalable IMs are the Peak Ground Acceleration (PGA), Peak Ground Velocity, the  $\xi = 5$  percent damped Spectral Acceleration in the structure's first-mode period ( $S_a(T_1; 5\%)$ ), and the normalized factor  $R = \lambda/\lambda_{yield}$  (where  $\lambda_{yield}$  signifies, for a certain record and structural model, the lowest scaling required to cause yielding) which is numerically equivalent to the yield reduction R-factor for, for instance, bilinear SDOF systems (see the next section). These IMs also have the characteristic of being proportional to the SF as they complete the relation. (Eq. 3.1)

$$IM_{prop} = \lambda \cdot f_{\vec{a}_1} \quad (3.1)$$

On the other hand the quantity:

$$S_{am}(T_1, \xi, a, b, c) = [S_a(T_1, \xi)]^a [S_a(cT_1, \xi)]^b \quad (3.2)$$

Suggested by Shome and Cornell and Mehanny is scalable and monotonic but non-proportional, unless  $b + d = 1$ .

Definition 3: Damage Measure (DM) or Structural State Variable is a non-negative scalar  $DM \in [0; +\infty]$  that represents the additional response of the structural model because of a prescribed seismic loading.

To state the matter differently, a DM is an observable quantity which is a part of, or can be inferred from, the yield of the related nonlinear dynamic analysis. probable choices could be peak storey ductility, maximum base shear, , various proposed damage indices (such as a global cumulative hysteretic energy, a global Park–Ang index or the stability index suggested by Mehanny), node rotations, peak roof drift, the floor peak inter-storey drift angles  $\theta_1, \dots, \theta_n$  of an n-storey structure, or their maximum, the maximum peak inter-storey drift angle  $\theta_{max} = \max(\theta_1, \dots, \theta_n)$ . Selecting an appropriate DM depends on the usage and the structure itself; it may be favourable to use two or more DMs (all caused by identical nonlinear analyses) to evaluate various response properties, limit-states or modes of failure of interest in a PBEE assessment. If the damage to non-structural contents in a multi-storey frame requires to be evaluated, the peak floor accelerations are the clear selection. However, since the structural damage of frame buildings,  $\theta_{max}$  relates to joint rotations and global and local storey collapse, hence it becomes a firm DM candidate. The second one, stated in the form of the total drift, instead of the efficient drift which would consider the building tilt, would be our selection of DM for many of the explanatory cases here, in which the foundation rotation and column shortening are not serious.

Definition 4: A Single-Record Ida Study is a dynamic analysis investigation of a certain structural model characterized by the scale factor of the certain ground motion time history.

This is also called the Incremental Dynamic Analysis (IDA) or Dynamic Pushover(DPO), and involves a series of dynamic nonlinear runs conducted under scaled pictures of an accelerogram, whose IMs are perfectly chosen to cover the

whole domain from elastic to nonlinear and eventually to the structure's collapse. The aim is to record DMs of the structural model in each level IM of the scaled ground motion, and the final response values is usually plotted versus the intensity level as continuous curves.

### 3.2.3 Capacity and Limit-States on Single IDA Curves

Levels of performance or limit states are crucial parts of Performance Based Earthquake Engineering (PBEE), and the IDA curve includes the essential data for analysing them. However, we require to explain them in a more concrete way that is reasonable on an IDA curve, for example by an expression or a code that when observed, signals reaching a limit-state. For instance, Immediate Occupancy is a structural performance level which is associated with acquiring a certain DM value, often in  $\theta_{max}$  terms, while (in FEMA 350, at least) Global Collapse is associated with the IM or DM value where dynamic instability is satisfied. A pertinent issue that emerges is what we should do when several points satisfy this rule? Which one should be chosen?

The reason for multiple points which are able to satisfy a limit-state rule is chiefly the toughening issue and, in its farthest form, structural resurrection. Generally speaking, we would want to be cautious and take into account the lowest, in IM terms, point which will show the limit-state.

Considering this, let's express the most fundamental rules which are used for defining a limit-state. First of all, the DM-based rule, produced from an expression of the format: "If  $DM \geq C_{DM}$  then the limit-state is passed. The fundamental idea is often that DM is a damage indicator, thus, when it goes beyond a given value the structural model is supposed to be in the limit-state. These  $C_{DM}$  values may be

achieved by experiment, theory or engineering experience, and they might not be deterministic, rather they may have the probability distribution. One instance could be the method that Mehanny and Deierlein (2000) used, in which a kind of structure-specific damage index is utilized as DM and in the point that its counterpart is larger than unity, the collapse is supposed to happen. An advantage of the DM-based rules is the plainness and easy implementation, specifically for performance levels except the collapse.

The alternative IM-based rule, is mostly produced from the requirement for better evaluation of the collapse capacity, by indicating a single point on the IDA curve which obviously divides that into two regions, a non-collapse one (lower IM) and a collapse one (higher IM). In monotonic IMs, this rule is created by an expression of the form: "If  $IM \geq C_{IM}$  and then the limit-state are passed. A significant distinction from the previous classification is the hardness of prescribing a  $C_{IM}$  value which signals the collapse for IDA curves, therefore it must be done separately and curve by curve. Nevertheless, the positive point is that it obviously produces one collapse region, and the negative point is the hardness of finding this point in each curve in a coherent manner. Generally speaking, this rule leads to *IM* and *DM* descriptions of capacity. A specific (or extreme) case could be considering the curve's final point as the capacity, i.e. by making use of the (lowest) flat line for defining the capacity (in *IM* terms), where all IDA curves before the emergence of dynamic instability are regarded as non-collapse.

The FEMA 20% tangent slope model is practically an *IM*-based rule; the final point on the curve which has a tangent slope of 20% of the elastic slope is considered as the capacity point. In this model, the curve's flattening represents the dynamic

instability (the  $DM$  raising in higher rates and hastening toward infinity). Because infinity cannot be a probable numerical result, we are satisfied with turning back to a rate of  $\theta_{max}$  increase which is equal to five times the initial or elastic rate, as the place that we show the capacity point. We must be careful that the probable weaving of an IDA curve may produce various points like this in which the structure appears to move towards the collapse, and it just recovers in a relatively higher  $IM$  level; basically, these low points must be therefore rejected as the capacity candidates.

The aforesaid simple rules are the constituent elements for building some composite rules, or the composite rational clauses like above, which are frequently connected by logical OR operators. For instance, when a structure has various collapse manners, which cannot be recognized by a single  $DM$ , it is useful to recognize the global collapse with an OR expression for each of the manners. In  $IM$  terms, the first occurrence that happens is the one that dominates the collapse capacity. One other case is the Global Collapse Capacity, defined by FEMA as an OR conjunction of the 20% slope  $IM$  -based rule and a  $C_{DM} = 10\%$   $DM$  -based rule, where  $S_a(T_1; 5\%)$  and  $\theta_{max}$  are the  $IM$  and  $DM$  of choice. In case each of the two rules obtains, it will define the capacity. It means that the 20% stiffness recognized the approaching collapse, while the 10% cap protects against excessive values of  $\theta_{max}$ , representing the regions that the model may not be reliable. It is a general remark for the collapse capacity; apparently it can be well expressed in  $IM$  terms.

#### **3.2.4 Multi-Record IDAs and Their Summary**

As should be evident by now, a single-record IDA study cannot fully capture the behaviour a building may display in a future event. The IDA can be highly dependent on the record chosen, so a sufficient number of records will be needed to cover the

full range of responses. Hence, we have to resort to subjecting the structural model to a suite of ground motion records.

Definition 5: A Multi-Record IDA Study is a collection of single-record IDA studies of the same structural model, under different accelerograms.

Such a study correspondingly produces sets of IDA curves, which by sharing a common selection of IMs and the same DM, can be plotted on the same graph.

Definition 6: An IDA Curve Set is a collection of IDA curves of the same structural model under different accelerograms that are all parameterized on the same IMs and DM.

While each curve, given the structural model and the ground motion record, is a completely defined deterministic entity, if we wish to take into account the inherent randomness with respect to what record the building might experience, we have to bring a probabilistic characterization into play. The IDA given the structural model and a statistical population of records is no longer deterministic; it is a random line, or a random function  $DM=f(IM)$  (for a single, monotonic IM). Then, just as we are able to summarize a suite of records by having, for example, mean, median, and 16%, 84% response spectra, so we can define mean, median and 16%, 84% IDA curves to (marginally) summarize an IDA curve set. We, therefore, need methods for estimating statistics of a sample of 2D random lines (assuming a single IM), a topic of Functional Data Analysis (Ramsay JO, Silverman BW, 1996). They conveniently fall in two main categories.

First are the parametric methods. In this case, a parametric model of the DM given the IM is assumed, each line is separately fit, providing a sample of parameter values, and then statistics of the parameters are obtained. Alternatively, a parametric model of the median DM given the IM can be fit to all the lines simultaneously. As an example, consider the two-parameter, power-law model  $\theta_{\max} = \alpha [S_a(T_1; 5\%)]^\beta$  introduced by Shome and Cornell (1999), which under the well-documented assumption of lognormality of the conditional distribution of  $\theta_{\max}$  given  $S_a(T_1; 5\%)$ , often provides a simple yet powerful description of the curves, allowing some important analytic results to be obtained (Jalayer F, Cornell CA., 2000; Cornell CA et al, 2002). This is a general property of parametric methods; while they lack the flexibility to accurately capture each curve, they make up by allowing simple descriptions to be extracted.

On the other end of the spectrum are the non-parametric methods, which mainly involve the use of ‘scatterplot smoothers’ like the running mean, running median, LOESS or the smoothing spline (Hastie TJ, Tibshirani RJ., 1990). Perhaps the simplest of them all, the running mean with a zero-length window (or cross-sectional mean), involves simply calculating values of the DM at each level of IM and then finding the average and standard deviation of DM given the IM level. This works well up to the point where the first IDA curve reaches capacity, when DM becomes infinite, and so does the mean IDA curve. Unfortunately, most smoothers suffer from the same problem, but the cross-sectional median, or cross-sectional fractile is, in general, more robust. Instead of calculating means at each IM level, we now calculate sample medians, 16 and 84% fractiles, which become infinite only when collapse occurs in 50, 84 and 16% of the records, respectively. Another advantage is

that under suitable assumptions (e.g. continuity and monotonicity of the curves), the line connecting the  $x\%$  fractiles of DM given IM is the same as the one connecting the  $(100-x)\%$  fractiles of IM given DM. Furthermore, this scheme fits nicely with the well-supported assumption of lognormal distribution of  $\theta_{max}$  given  $S_a(T_1; 5\%)$ , where the median is the natural ‘central value’ and the 16%, 84% fractiles correspond to the median times  $e^{\mp dispersion}$ , where ‘dispersion’ is the standard deviation of the logarithms of the values (Jalayer F, Cornell CA, 2000).

Finally, a variant for treating collapses is proposed by Shome and Cornell (2000), where the conventional moments are used to characterize non-collapses, thus removing the problem of infinities, while the probability of collapse given the IM is summarized separately by a logistic regression. A simpler, yet important problem is the summarizing of the capacities of a sample of  $N$  curves, expressed either in DM (e.g.  $\{C_{\theta_{max}}^i\}, i = 1 \dots N$ ) or IM (e.g.  $\{C_{S_a(T_1; 5\%)}^i\}, i=1 \dots N$ ) terms. Since there are neither random lines nor infinities involved, the problem reduces to conventional sample statistics, so we can get means, standard deviations or fractiles as usual. Still, the observed lognormality in the capacity data, often suggests the use of the median (e.g.  $\hat{C}_{S_a(T_1; 5\%)} or \hat{C}_{\theta_{max}}$ ), estimated either as the 50% fractile or as the antilog of the mean of the logarithms, and the standard deviation of the logarithms as dispersion. Finally, when considering limit-state probability computations; one needs to address potential dependence (e.g. correlation) between capacity and demand. Limited investigation to date has revealed little if any systematic correlation between DM capacity and DM demand (given IM).

### 3.3 Operational Damage Levels

According to ATC-40, FEMA-356 and SEAOC (2000), we can say that, determination of operational objectives is a combination of expected hazard level and operational level. We would have 4 parts in operational level (SEAOC 2000) as follows:

- Fully Operational: Continuous service; negligible structural and non-structural damage. Considered for frequent occurrence.
- Immediate Occupancy: Sustain minimal or no damage to the structural elements and only minor damage to the nonstructural components. Considered for occasional occurrence.
- Life Safe: Damage is moderate or high; Life safety is generally protected. Considered for relatively strong earthquakes
- Near Collapse: Damage severe, but structural collapse prevented. Considered for high intensive earthquakes and there is life safety risk at this level.

An operational level (apart from those of SEAOC 2000) is introduced for this study named dynamic instability at which collapse is occurred.

Table 3.1. Hazard level (SEAOC 2000)

Earthquake Classification	Recurrence Interval	Probability of Occurance
Frequent	43 years	50% in 30 years
Occasional	72 years	50% in 50 years
Rare	475 years	10% in 50 years
Very Rare	970 years*	10% in 100 years

And (BSSC 1998) added a new hazard level in accordance with MCE (with a recurrence interval of 2475 years and 2% chances of occurrence in 50 years).

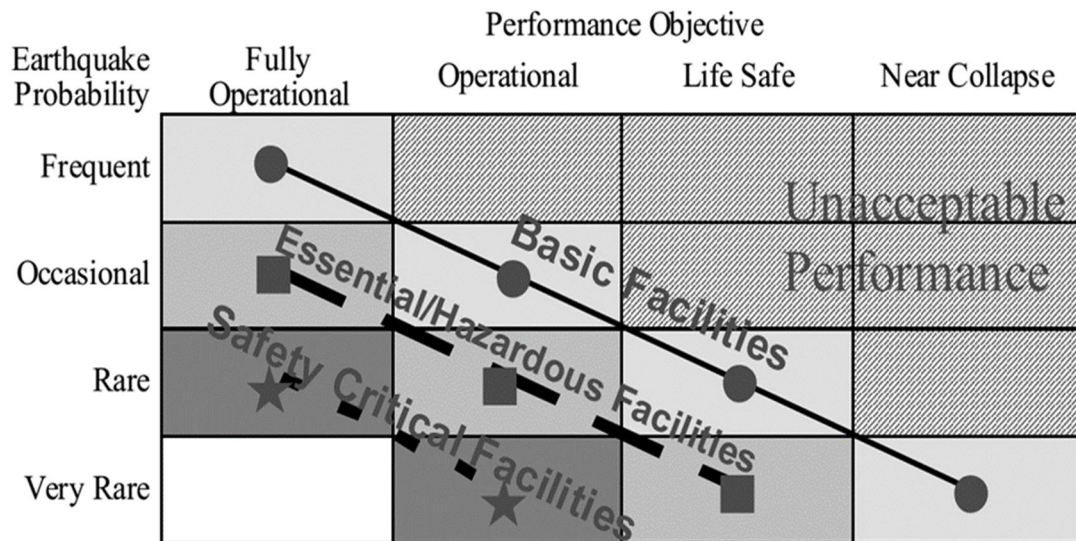


Figure 3.1. Operational levels matrix (SEAOC 2000)

Table 3.2. Hazard and operational levels ATC-40, FEMA-356

		Target Building Performance Levels*			
		Operational Performance Level (1-A)	Immediate Occupancy Performance Level (1-B)	Life Safety Performance Level (3-C)	Collapse Prevention Performance Level (5-E)
<b>Earthquake Hazard Level (ground motions having a specified probability of being exceeded in a 50-year period)</b>	50%/50 year	a	b	c	d
	20%/50 year	e	f	g	h
	BSE-1 (10%/50 year)	i	j	k	l
	BSE-2 (2%/50 year)	m	n	o	p

\*Alpha-numeric identifiers in parentheses defined in Table 4-2

**Notes:**

- Each cell in the above matrix represents a discrete Rehabilitation Objective
- Three specific Rehabilitation Objectives are defined in FEMA 356:
  - Basic Safety Objective = cells k + p
  - Enhanced Objectives = cells k + p + any of a, e, i, b, f, j, or n
  - Limited Objectives = cell k alone, or cell p alone
  - Limited Objectives = cells c, g, d, h, l

Two last rows are safe design levels with recurrence interval of 747 and 2475 years.

Obviously the more desirable performance objectives cause additional costs.

Determination the structural performance of a building depends on several parameters. If the desired performance goals are known before, performance and hazard levels can be expected to be well known. However, there is a need to introduce trustworthy parameters for structural analysis (relative deformation, plastic cycles, formation ...).

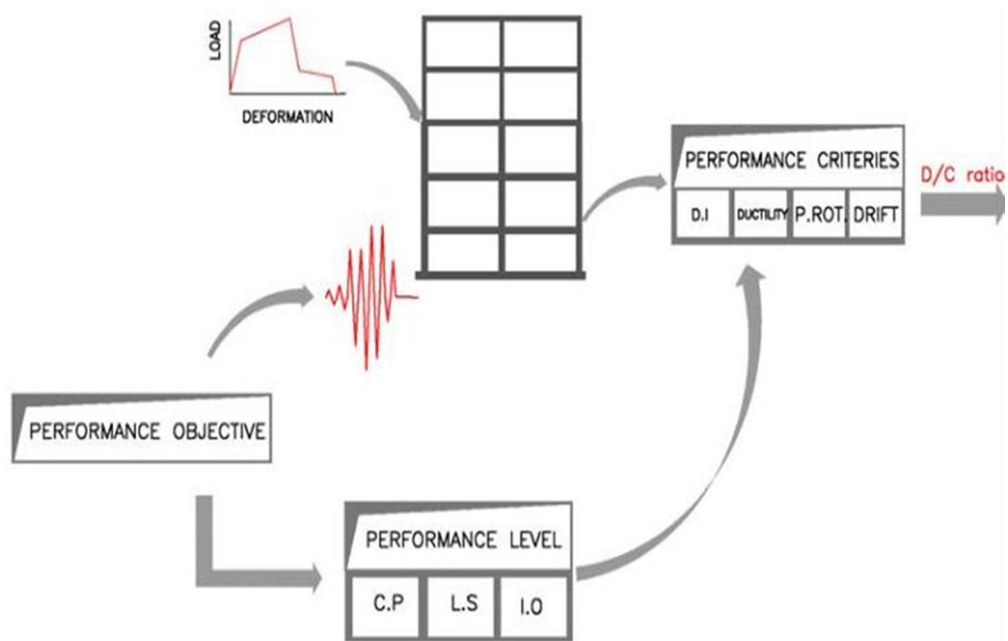


Figure 3.2. Associated components involved in structural performance evaluation (Khanmohammadi, 2005)

### 3.4 Confidence Level of Global Collapse

Confidence parameter ( $\lambda$ ) is used to determine the confidence level and obtained via the ratio of factored demand to capacity (Eq. 3.3).

$$\lambda = \frac{\gamma \cdot \gamma_a \cdot D}{\phi \cdot C} \quad (3.3)$$

- $D$  Median drift demand
- $C$  Median drift capacity
- $\phi$  Resistance factor
- $\gamma$  Demand uncertainty factor

$\gamma_a$  Analysis uncertainty factor

$\gamma_a$ ,  $\gamma$  and  $\phi$  factors are based on a reliability-based framework adopted by the SAC project and advanced by Jalayer and Cornell (2002). Following on, the procedure to evaluate these parameters for all structural systems is presented. More details are provided by Jalayer and Cornell (2002) as well as Cornell et al (2002).

#### **3.4.1 Median Drift Demand (D)**

Each building for each ground motion record is analysed using a nonlinear analysis. Maximum drift demand for each building and for each of the records is obtained. The median of maximum drift demand for a building is considered as demand.

#### **3.4.2 Median Drift Capacity (C)**

This parameter can be found by making use of the incremental dynamic analysis developed by Vamvatsikos and Cornell (2002), which was used in SAC. The median of drift capacity of global collapse is considered as capacity.

#### **3.4.3 Resistance Factor ( $\phi$ )**

This parameter is calculated from testing for local collapse and from IDA for global collapse and known as resistance factor of building elements.

The factor of resistance,  $\phi$ , explains the event that the structural capacity includes value distribution. With the purpose of determining the levels of confidence and possibilities, this variation's sources are divided into randomness and uncertainty. The main part of randomness in global capacity results from the variation in the earthquake accelerograms that a building can experience (which was indicated by accelerograms suite utilized in the IDA analyses). In addition, estimating the capacity also faces the uncertainty in load- the system's deformation behaviour, which could be basically determined through tests. The local collapse value is also influenced by

uncertainty in the components' response because of changeable material characteristics as well as fabrication. The formula for calculating  $\varphi$  is proposed by Cornell et al (2002).

$$\varphi = \varphi_{RC} \varphi_{UC} \quad (3.4)$$

$$\varphi_{RC} = e^{-k\beta_{RC}^2/2b} \quad (3.5)$$

$$\varphi_{UC} = e^{-k\beta_{UC}^2/2b} \quad (3.6)$$

- $\varphi_{RC}$  Contribution to  $\varphi$  from randomness of earthquake accelerogram.
- $\varphi_{UC}$  Contribution to  $\varphi$  from uncertainties in measured connection capacity.
- $\beta_{UC}$  Standard deviation of the natural logs of the drift capacities due to randomness, obtained from the testing.
- $\beta_{RC}$  Global collapse Standard deviation of natural logs of drift capacities due to uncertainty, determined using the IDA procedure, independent of the uncertainties in demand.  
Local collapse Equal to the variability observed in cyclic capacity, obtained from experimental tests; not considered in this study.
- $b$  Typically taken as having a value of 1.0 (Cornell, 1999; FEMA355F, 2000).
- $k$  The slope of the hazard curve provided by USGS (Foutch, 2000).

In case of the local collapses,  $\beta_{UC}$  represents the uncertainty in median drift capacity. This results from the uncertainties in representativeness of the process of testing, in the restricted number and scope of tests, material, and weld characteristics, as well as some other factors. The  $\beta_{RC}$  term represents the randomness of drift capacity which is mainly due to the record dependent variations in the story drift (or connection rotation) in collapses.

The slope of hazard curve ( $k$ ) is readily calculated from data given by the USGS (Foutch, 2000).  $b$  parameter is associated with the rate of change in capacity to the

rate of change in demand. It had a value of 1 for SAC; but it may be different for other buildings and systems (Cornell et al, 2002).

Capacities determined from testing are subject to uncertainties.  $\beta_{UC} = 0.25$  has a good value and was once used in SAC. All  $\beta$  values that will be referred later, shows standard deviations relating to variation in storey-drift.

#### 3.4.4 Determining the Slope of Hazard Curve (k)

In fact, the slope of the hazard curve is a function of hazard level, location and response period. The hazard curve is a scheme of the possibility of exceedance of a spectral amplitude value versus the spectral amplitude for a certain response period, and is frequently nearly linear when it is drawn on a log-log scale (Eq. 3.7).

$$H_{S_i}(S_i) = k_0 S_i^{-k} \quad (3.7)$$

If mapped spectral acceleration values at 10%/50 year and 2%/50 year exceedance possibilities are available, the k value can be calculated as Eq. 3.8.

$$k = \frac{\ln \left[ \frac{H_{Sa}(Sa_{10\%})}{H_{Sa}(Sa_{2\%})} \right]}{\ln \left[ \frac{Sa_{2\%}}{Sa_{10\%}} \right]} \quad (3.8)$$

$S_{1(10/50)}$  = Spectral amplitude for 10/50 hazard level

$S_{1(2/50)}$  = Spectral amplitude for 2/50 hazard level

$H_{S_{1(10/50)}}$  = Probability of exceedance for the 10/50 hazard level =  $1/475 = 0.0021$

$H_{S_{1(2/50)}}$  = Probability of exceedance for the 2/50 hazard level =  $1/2475 = 0.00040$

The default  $k$  values for different areas in the United States and  $i$ = Desired period (for  $S_5$  equals to 0.3 and for  $S_1$  equals 1).

USGS maps supply values of 5%-damped, spectral response accelerations in 0.2 seconds periods, termed  $S_S$ , and 1 second, termed  $S_1$ , for ground motions having 2% and 10% possibilities of exceedance in 50 years, for all regions in the United States.

### 3.4.5 Determination of $\gamma$

Similar to the resistance factor, demand factor ( $\gamma$ ) is also vulnerable to the effects of randomness and uncertainty. This randomness results from the unforeseeable difference in the real ground motion accelerogram and also from the difference in the azimuth of attack, called orientation, of the ground motion.

Uncertainty arises from the nonlinear dynamic analysis method. This coefficient was proposed, for steel building with moment frame system of 3, 9 and 20 storeys respectively, 0.15, 0.2 and 0.25. As said, demand coefficient ( $\gamma$ ) is influenced from randomness arising from earthquake accelerograms.

The orientation element is an important factor merely for the near-fault site. For these sites which are within a few kilometres of the fault rupture zone, the fault-parallel and fault-normal directions endure completely different shaking. For places that are far away from the fault, there exists no statistical variation in the accelerograms recorded in various directions.

Uncertainties of earthquake accelerograms arises from calculating the logarithmic changes of maximum drift computed for each of the different accelerograms.

$$\gamma = e^{k\beta_{RD}^2/2b} \quad (3.9)$$

$$\beta_{RD} = \sqrt{\sum \beta_i^2} \quad (3.10)$$

Here  $\beta_i^2$  is the variance of the natural log of the drifts for every component of randomness. The  $\beta_i$  values for the sources of randomness include:  $\beta_{acc}$  , accelerogram;  $\beta_{or}$  , orientation.  $\beta_{acc}$  is the standard deviation of the log of the maximum story drifts computed for every chosen accelerogram. The operant “” is just considered for near-field sites of California which have known faults. So for far-field sites  $\beta_{RD} = \beta_{acc}$ .

### 3.4.6 Determination of $\gamma_a$

The factor of demand uncertainty  $\gamma_a$  depends on uncertainties of determination of the median demand  $D$ .  $\beta$  values for each of the sources of uncertainty are as to what the project SAC (Yun and Foutch, 2000) and hazard curves 2%/50 and 50%/50 is. These values are based on the investigation of three buildings which were designed on the basis of UBC and twenty buildings according to NEHRP for the Los Angeles area. And the symbol used to show that is  $\beta_a$ .

An important uncertainty source results from the impreciseness of the analytical process, called  $\beta_a$  for the analysis procedure. The  $\beta_a$  is somehow composed of four segments which include:  $\beta_{NTH}$  related to uncertainties of the extent that the benchmark, nonlinear time history analysis procedure, indicates the real physical behaviour;  $\beta_{damping}$  related to uncertainty of estimating the structure's damping value;  $\beta_{live\ load}$  related to the uncertainty in the live load;  $\beta_{mat.prop.}$  related to the uncertainty of material characteristics (Yun and Foutch, 2000).

Only  $\beta_{NTH}$  and  $\beta_{damping}$  are large enough to be considered in the structure with steel moment frame. For other materials, and other systems are all sources of uncertainty may be considered. Attenuation values measured in structure tests in full scale is

required to calculate  $\beta_{damping}$ . Sufficient data for this parameter is only available for steel and concrete moment frames, steel braced frames as well as the reinforced concrete buildings with shear walls.  $\beta_{live\ load}$  may not be important for commercial and residential buildings. This parameter may be important for warehouses and buildings that have live load. The calculation of  $\beta$  is relatively complex (Yun and Foutch, 2000). In this study,  $\beta_{NTH}$  is merely considered and obtained from proposed values of FEMA-355F.

### 3.4.7 Calculation of $\beta_{UT}$

$\beta_{UT}$  is a function of all uncertainties. The utilized uncertainty coefficient values  $\beta_{UT}$  depend on some uncertainty sources in estimating the structural demands and capacities. Therefore, this parameter does not consider randomness.

$$\beta_{UT} = \sqrt{(\beta_U^2 + \beta_a^2)} \quad (3.11)$$

### 3.4.8 Calculation of Confidence Parameter ( $\lambda$ )

Confidence parameter  $\lambda$ , is dependent on the slope  $k$  of hazard curve and uncertainties due to the natural logarithm of the drifts (Jalayer and Cornell, 2002).

$$\lambda = e^{-\beta_{UT}(K_x - k\beta_{UT}/2b)} \quad (3.12)$$

$K_x$  = Standard Gaussian variate related to the possibility  $x$  of not being exceeded discovered in the customary probability tables. Confidence parameter can be written as a function of  $K_x$ .

$$K_x = \left[ -\ln(\lambda) + \frac{1}{2b} \cdot k \cdot \beta_{UT}^2 \right] \cdot \frac{1}{\beta_{UT}} \quad (3.13)$$

The order to compute the confidence level is as follows:

- Calculation of confidence parameter.
- Calculation of  $K_x$ .
- Calculation of confidence level from statistical books.

Reverse of this procedure can properly be applied to the design process.

- Determination of confidence level for structure.
- Calculation of drift demand to accompany with the confidence level.

As  $\lambda$  is factored-demand-to-capacity ratio, confidence level increases if  $\lambda$  decreases.

### **3.5 Construction of Fragility Curves**

#### **3.5.1 Overview of Fragility Curves**

Existing vulnerability curves can be categorized into four generic groups which are: empirical, judgmental, analytical and hybrid based on whether the damage data utilized in their creation derives chiefly from the observed post-earthquake tests, expert opinion, analytical simulations, or respectively a mixture of these.

- Empirical curves
- Judgment-based curves
- Analytical vulnerability curves
- Hybrid vulnerability curves

The empirical curves utilize the building damage distributions reported in the investigations after the earthquake as their statistical foundation. The observational source is the most realistic when all functional specifications of the stock are considered besides soil–structure interaction impacts, site, topography, path and source characteristics. Although, these aspects that make the observational data realistic also account for the serious limitation in their potential of application (Rossetto and Elnashai, 2003; Orsini, 1999).

Judgement-based curves are not related the same problems of the quantity and quality of building damage statistics that represent the empirical connections. The reliability of judgement based curves can be questioned, although, because of their dependence on the individual experience of the consulted experts (HAZUS and ATC-13).

Analytical susceptibility curves adopt damage distributions which are simulated from the structural models analyses in increasing earthquake loads for their statistical foundation. Analyses may lead to less bias and increased reliability of the susceptibility estimate for various structures in comparison to the expert opinion (Reihorn et al, 2001; Ramamoorthy et al, 2006).

The hybrid susceptibility curves try to make up for the observational data rareness, judgemental data subjectivity and modelling deficiencies of analytical processes by mixing the data from different sources. Current instances of the hybrid curves usually include the modification of analytical or judgement based relations with the observational information (Kircil and Polat, 2006; Singhal and Kiremidijan, 1998).

### **3.5.2 Uncertainties Effects on Fragility Curves**

Generally, uncertainties are divided into two parts (Wen et al, 2003).

- Inherent uncertainty that are due to elements that are essentially random (or inherent) for understanding in engineering. In this study, uncertainties are related to materials and earthquake records.
- Epistemic uncertainty which arises from the absence of knowledge, unawareness or modeling assumptions and are case dependent.

In this study, the uncertainty is discussed at inherent level. So uncertainties in fragility curves are discussed at the following levels:

A: Uncertainty in the structure itself is separable into two parts:

A1: Uncertainty in material properties.

A2: Uncertainty in Structural Dynamics Profile (beam and column dimensions and mass of the structure) and uncertainty in the geometry of the structures.

B: Uncertainty in earthquake

## Chapter 4

### THE PROPOSED METHOD

#### 4.1 Introduction

One important subject studied by earthquake engineers as part of a performance-based approach is the determination of demand and collapse capacity under earthquake. Different methods for evaluating seismic structural performance have been suggested along with and as part of the development of performance-based earthquake engineering.

Sufficient amount of demand-illustrator curves derived from different intensities of ground motions are provided for high quantity of earthquakes; in order to assess the operational results of buildings statistically. Average and response dispersion are available via these curves, and accordingly a demand value corresponding to a desired probability can be obtained (e.g. probability of 84% defines a demand value for a selected ground motion such that the demand quantity is less than the specified value based on 84% probability); such an analysis would introduce hazard curves in which the probability of increasing the annual average of demand relative to it is specified value will be shown. This method, if matured, could have considerable benefits in estimating seismic demands in performance-based engineering.

Although such an approach requires a large number of inelastic time history analyses, it has been used by several researchers for different applications. Different

approximate methods have also emerged, aiming at reducing computational effort. The approximate methods for IDA analysis usually involve the replacement of nonlinear dynamic analysis by a combination of the pushover analysis of a structural model and dynamic analysis of a simple model, e.g. SDOF model. However, if it is a requirement that the seismic response of a structure is predicted with the most accurate nonlinear dynamic analysis, then the practical application of incremental dynamic analysis is limited mainly due to the computational effort needed to perform incremental dynamic analysis, but also due to the definition of the seismic loading, which is, in this case, defined by a set of ground motion records. Different questions arise in the process of selecting the ground motion records for the incremental dynamic analysis. Firstly it is important that the selected set of ground motion records reflects the seismic hazard of the particular site and that the scaling of records is “legitimate”. When these two conditions are not satisfied, a bias in the structural response can occur. However, careful selection of ground motion records can reduce the bias in the structural response.

Such an approach has been used by several researchers for different applications. Concluded that incremental dynamic analysis and its interpretation is accompanied by many problems, so we try out to challenge the complexities stated.

## **4.2 Buildings in the study**

Building models in this study consisted of a 6-storey building as a low-rise, a 10-storey building as a mid-rise and a high-rise building of 15 floors. Plan and elevation view of the buildings are shown at Figures 4.1 and 4.2. The overall height of the buildings for 6, 10 and 15-storey are respectively 19.2 m, 32 m and 48 m. These buildings are designed to ACI 318 (American Concrete Institute, 2008) and ASCE 7

(American Society of Civil Engineers, 2005) standards. Compressive strength of concrete and yield strength of steel are 30 and 400 MPa respectively. At all storeys, uniform dead and live loads on the structure, are 6 and  $2kN/m^2$  respectively. In earthquake engineering, correction factor for the response of special reinforced concrete moment-resisting frame, in accordance with Guideline ASCE 7-05, is considered to be 8. The importance factor is equal to 1. Effective seismic weight includes the total dead load without involving the live load. Accidental torsion is considered equal to 5% of the dimension of the structure perpendicular to the direction of the applied earthquake forces. Following the requirements of guideline, dimensions of structural members such as beams, columns and shear walls and the steel used are specified. The columns have been placed in raft foundation to decrease translation and rotation at the footing to zero. At all floors, in ceiling systems, concrete slab thickness of 8 cm is considered. Members' specifications of the building models are listed in Table 4.1. Preliminary analysis has been done by finite element program; ETABS. The nonlinear evaluations are carried out using a typical two-dimensional frame from each of the buildings. The computer simulations are carried out using the open source finite-element platform, OpenSees. A force-based nonlinear displacement beam-column element that utilizes a layered "fibre" section is utilized to model all components of the frame models.

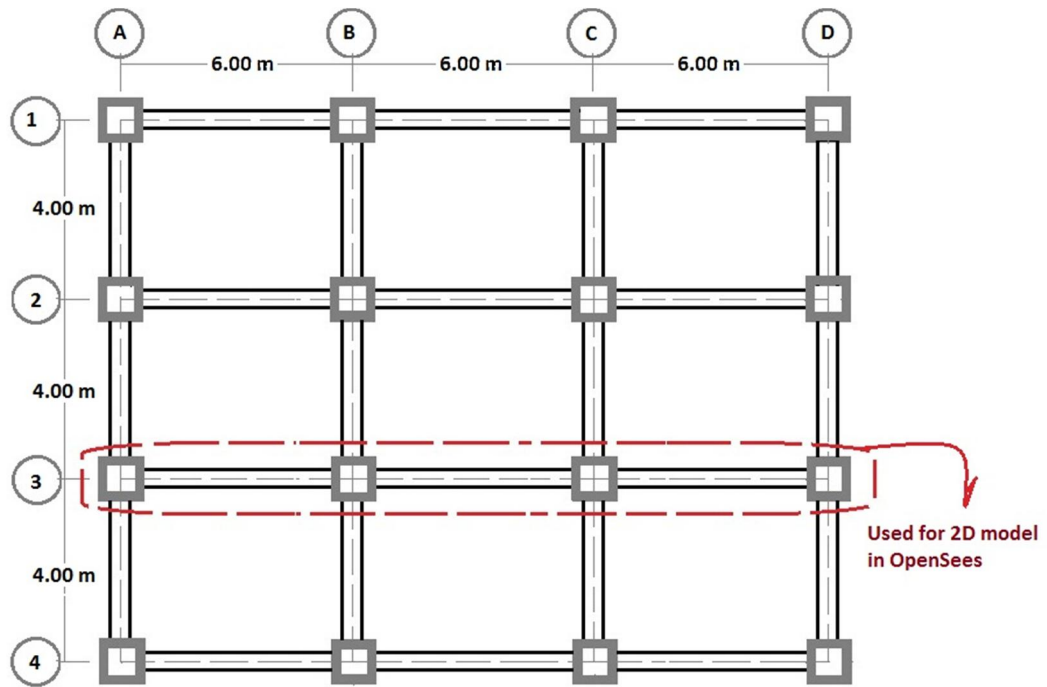


Figure 4.1. Building models-Plan

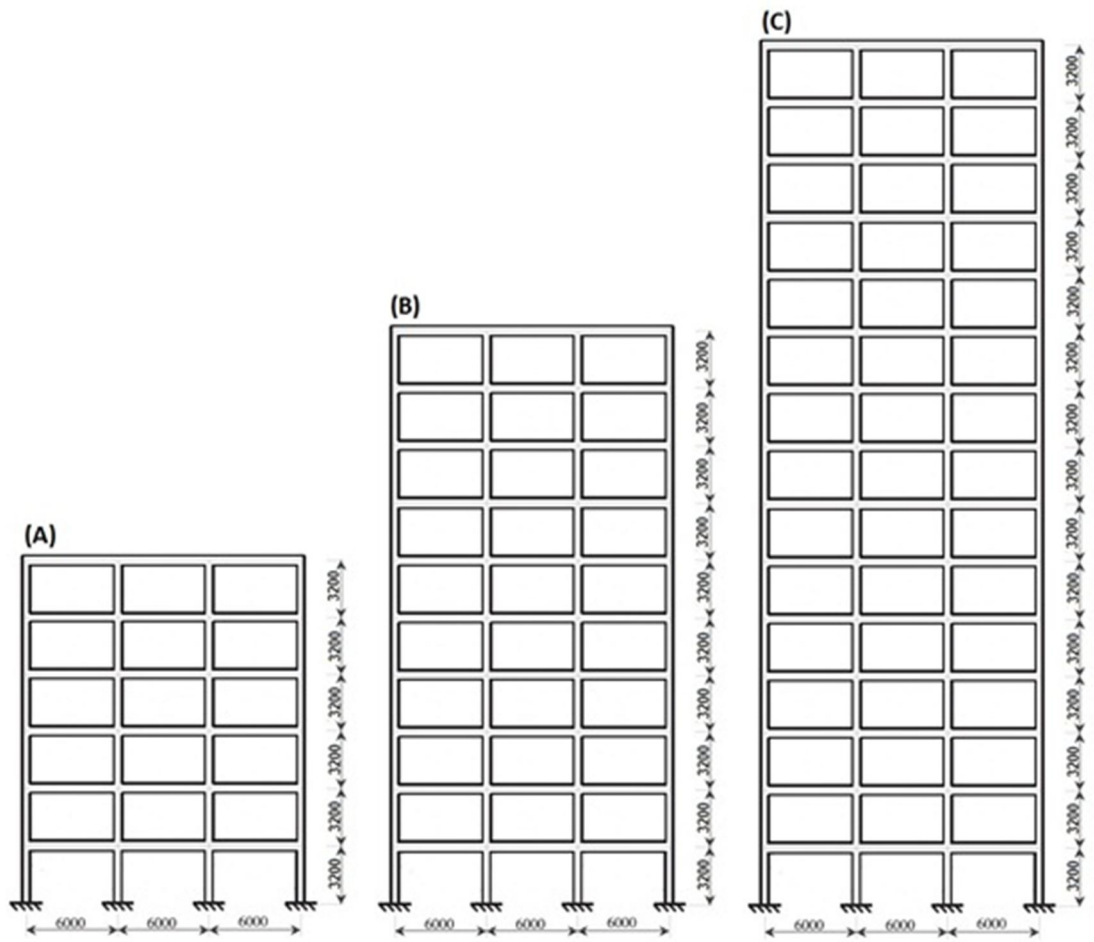


Figure 4.2. Building models-Elevation view; a) 6-story b) 10-story c) 15-story

Table 4.1. Columns' and Beams' sections specifications

Models	Storey	Column		Storey	Beam		
		Size	Reinf.		Size	Top Reinf.	Bot Reinf.
6 Storey	5,6	60x60	32 $\Phi$ 20	1-3	60x40	3 $\Phi$ 20	3 $\Phi$ 20
	3,4	50x50	20 $\Phi$ 20	4-6	50x40	3 $\Phi$ 20	3 $\Phi$ 20
	1,2	40x40	12 $\Phi$ 20				
10 Storey	1	70x70	40 $\Phi$ 20	1-6	65x40	3 $\Phi$ 20	3 $\Phi$ 20
	2-4	60x60	32 $\Phi$ 20	7-10	55x40	3 $\Phi$ 20	3 $\Phi$ 20
	5-8	50x50	20 $\Phi$ 20				
	9,10	40x40	12 $\Phi$ 20				
15 Storey	1-5	70x70	40 $\Phi$ 20	1-10	70x40	3 $\Phi$ 20	3 $\Phi$ 20
	6-8	60x60	32 $\Phi$ 20	11-15	60x40	3 $\Phi$ 20	3 $\Phi$ 20
	9-12	50x50	20 $\Phi$ 20				
	13-15	40x40	12 $\Phi$ 20				

### 4.3 Performed analysis

Seismic performance of three 6, 10 and 15-story reinforced concrete buildings have been evaluated under 28 ground motion records with magnitudes over 6 Richter based on incremental dynamic analysis. Fourteen far-field and 14 near-field records are selected to perform a comprehensive assessment. Near-field records are selected in such a way that both forward-directivity, producing double-sided velocity pulses, and fling-step, characterized by one-sided velocity pulses (these pulses in turn causes a large static offset at the end of the displacement time-history), are included.

According to the analysis results, responses including shear profile at storeys, displacement profile of storeys, inter-storey relative displacement profile, mechanism of structure collapse and plastic joints formation, etc. are studied. Finally, an overall framework to interpret the seismic responses of reinforced concrete buildings is achieved.

According to these analyses, the following objectives are investigated:

- Survey on seismic shear distribution at stories based on near-fault and far-fault records.
- Survey on displacement profile of stories based on near-fault and far-fault records.
- Survey on how inter-story relative displacement profile changes (as the main source of destruction) based on near-fault and far-fault records.
- Survey on collapse mode based on near-fault and far-fault records.

It should be noted that the analyses of current study are conducted by OpenSees 2.02.

#### **4.4 Ground motion records and the analyses**

Tables 4.2 and 4.3, show the profile of earthquake records used in the present study which have been extracted of the database of Earthquake Engineering Research Centre, University of California Berkeley. As mentioned, 28 ground motion records have been used including 14 far-fields and 14 near-fields. Far-fields ground motions of 6.1 to 7.5 magnitudes at distances 50 to 115 km from the site and recorded on soft or firm soils are the first group of records. The second group involves near-fields ground motions of 6.6 and 7.6 magnitude recorded at distances 0.24 to 11 km from the site and on soft or firm soils. In Tables 1 and 2 specifications of the records, including the recording stations, seismic component, moment magnitude, distance to fault, peak ground acceleration (PGA), peak ground velocity (PGV) and peak ground displacement (PGD) are given.

Table 4.2. Specifications of near-fault ground motion records

Record No	Year	Earthquake	M <sub>w</sub>	Mech. <sup>1</sup>	Station	GM Characteristics	Dist. <sup>2</sup> (km)	Site Class <sup>3</sup>	DataSrc. <sup>4</sup>	Comp.	PGA (g)	PGV (cm/s)	PGD (cm)	Arias Intensity (m/sec)	dt (sec)
1	1999	Chi-Chi	7.6	TH	TCU052	Fling	1.84	D	4	EW	0.349	177.936	491.409	2.756696	0.005
2	1999	Chi-Chi	7.6	TH	TCU052	Fling	1.84	D	4	NS	0.438	215.881	704.840	2.8250629	0.005
3	1999	Chi-Chi	7.6	TH	TCU068	Fling	3.01	D	4	EW	0.501	277.616	718.005	3.175701	0.005
4	1999	Chi-Chi	7.6	TH	TCU068	Fling	3.01	D	4	NS	0.363	294.081	893.297	3.08941	0.005
5	1999	Kocaeli	7.4	SS	Sakarya	Fling	3.20	C	3	EW	0.415	81.957	205.924	1.88944	0.01
6	1999	Chi-Chi	7.6	TH	TCU072	Fling	7.87	D	4	NS	0.364	66.719	245.293	4.5900978	0.005
7	1999	Chi-Chi	7.6	TH	TCU128	Fling	9.08	C	4	EW	0.138	59.471	89.615	0.5810721	0.005
8	1999	Kocaeli	7.4	SS	Izmit	Fling	4.30	B	3	EW	0.233	48.864	95.487	0.9900877	0.005
9	1994	Northridge-01	6.69	REV	LA - Sepulveda VA Hospital	Fling	6.70	C	5	4C	0.464	13.798	26.128	1.531879	0.02
10	1994	Northridge-01	6.69	REV	Arleta - Nordhoff Fire Sta	Fling	3.30	D	1	UP	0.552	17.955	10.433	2.08477	0.02
11	1994	Northridge-01	6.7	REV	Rinaldi Receiving Sta	Fling	7.5	D	2	P	0.871	28.606	1.016	1.3484918	0.005
12	1994	Northridge-01	6.7	REV	Rinaldi Receiving Sta	Fling	7.5	D	2	N	0.387	10.060	0.477	0.5573578	0.005
13	1999	Chi-Chi	7.6	TH	TCU079	Fling	11.0	D	4	EW	0.568	68.053	166.099	7.1329861	0.005
14	1999	Chi-Chi	7.6	TH	TCU078	Fling	8.3	D	4	EW	0.431	41.876	121.222	5.3532219	0.005

<sup>1</sup> Faulting Mechanism = TH: Thrust; REV: Reverse; SS: Strike-slip; OB: Oblique; RN (Reverse-Normal), RO (Reverse-Oblique), NO (Normal-Oblique).

<sup>2</sup> Closest distance to fault rupture (i.e.,  $r_{fb}$ )

<sup>3</sup> NEHRP Site Classifications => (B for  $V_S = 760$  to  $1500$  m/s), (C for  $V_S = 360$  to  $760$  m/s), (D for  $V_S = 180$  to  $360$  m/s)

<sup>4</sup> Data Source = 1: PEER (<http://peer.berkeley.edu/smcat>); 2: Berkeley ([http://nisee.berkeley.edu/data/strong\\_motion/sacsteel/motions/nearfault.html](http://nisee.berkeley.edu/data/strong_motion/sacsteel/motions/nearfault.html));

3: ERD (<http://angora.deprem.gov.tr/>); 4: <http://scman.cwb.gov.tw/eqv5/special/19990921/pgadata-ascii0704.htm>

5: Buffalo ([https://mceer.buffalo.edu/info-service/reference\\_services/strongMotionGuide.asp](https://mceer.buffalo.edu/info-service/reference_services/strongMotionGuide.asp))

Table 4.3. Specifications of far-fault ground motion records

Record No	Year	Earthquake	M <sub>w</sub>	Mech. <sup>1</sup>	Station	GM Characteristics	Dist. <sup>2</sup> (km)	Site Class <sup>3</sup>	DataSrc. <sup>4</sup>	Comp.	PGA (g)	PGV (cm/s)	PGD (cm)	Arias Intensity (m/sec)	dt (sec)
1	1952	Kern county	7.5	TH/REV	Taft	Far-Fault	81.0	D	1	111	0.178	17.475	8.840	0.58627	0.01
2	1978	Tabas	7.4	TH/REV	Dayhook	Far-Fault	107		1	LN	0.400	26.174	9.097		0.005
3	1979	Imperial-Valley	6.5	SS	Calexico	Far-Fault	90.6	D	1	225	0.275	42.469	35.924	1.70186	0.01
4	1989	Loma Prieta	7.0	OB	Presidio	Far-Fault	83.1	D	1	0	0.099	12.911	4.324	0.153619	0.005
5	1989	Loma Prieta	6.9	RO	Cliff House	Far-Fault	84.40	A	1	90	0.107	19.780	5.060	0.36784	0.005
6	1990	Manjil	7.4		Abbar	Far-Fault	74.00		1	L	0.510	42.460	14.918		0.01
7	1999	Kocaeli	7.4		Ambarli	Far-Fault	78.90	C	1	90	0.179	33.222	25.840		0.02
8	1994	Northridge	6.7	TH	La-Puente	Far-Fault	56.60	D	1		0.129	9.656	0.824	0.18026	0.01
9	1994	Northridge	6.7	TH	Baldwin-Park	Far-Fault	47.70	D	1		0.123	8.170	1.326	0.11929	0.01
10	1992	Landers	7.3	SS	Baker	Far-Fault	87.90	D	1		0.108	9.329	6.255	0.239656	0.02
11	1952	Kern county	7.5	TH/REV	SantaBarbara Courthouse	Far-Fault	114.60	B	1		0.127	15.447	4.134	0.25066	0.01
12	1986	N. Palm Springs	6.2	SS	Temecula	Far-Fault	64.70	D	1		0.121	6.880	0.549	0.093535	0.005
13	1986	N. Palm Springs	6.2	SS	Anza Tule Canyon	Far-Fault	51.90	D	1		0.110	6.541	0.711	0.059725	0.005
14	1987	Whittier-Narrows	6.1	TH/REV	Glendora	Far-Fault	63.80	D	1		0.110	4.871	0.805	0.1029511	0.02

<sup>1</sup> Faulting Mechanism = TH: Thrust; REV: Reverse; SS: Strike-slip; OB: Oblique; RN (Reverse-Normal), RO (Reverse-Oblique), NO (Normal-Oblique).

<sup>2</sup> Closest distance to fault rupture (i.e.,  $r_{fb}$ )

<sup>3</sup> NEHRP Site Classifications => (B for  $V_S = 760$  to  $1500$  m/s), (C for  $V_S = 360$  to  $760$  m/s), (D for  $V_S = 180$  to  $360$  m/s)

<sup>4</sup> Data Source = 1: PEER (<http://peer.berkeley.edu/smcat>); 2: Berkeley ([http://nisee.berkeley.edu/data/strong\\_motion/sacsteel/motions/nearfault.html](http://nisee.berkeley.edu/data/strong_motion/sacsteel/motions/nearfault.html));

3: ERD (<http://angora.deprem.gov.tr/>); 4: <http://scman.cwb.gov.tw/eqv5/special/19990921/pgadata-ascii0704.htm>

5: Buffalo ([https://mceer.buffalo.edu/infoservice/reference\\_services/strongMotionGuide.asp](https://mceer.buffalo.edu/infoservice/reference_services/strongMotionGuide.asp))

For nonlinear time history analysis, ground motions were scaled to the spectrum consistent with ASCE 7-05 standard design range with 5% damping and the minimum error in the time range of 0.6 to 4 seconds. Hence, the average of 14 records per group of ground motions provides an acceptable design range.

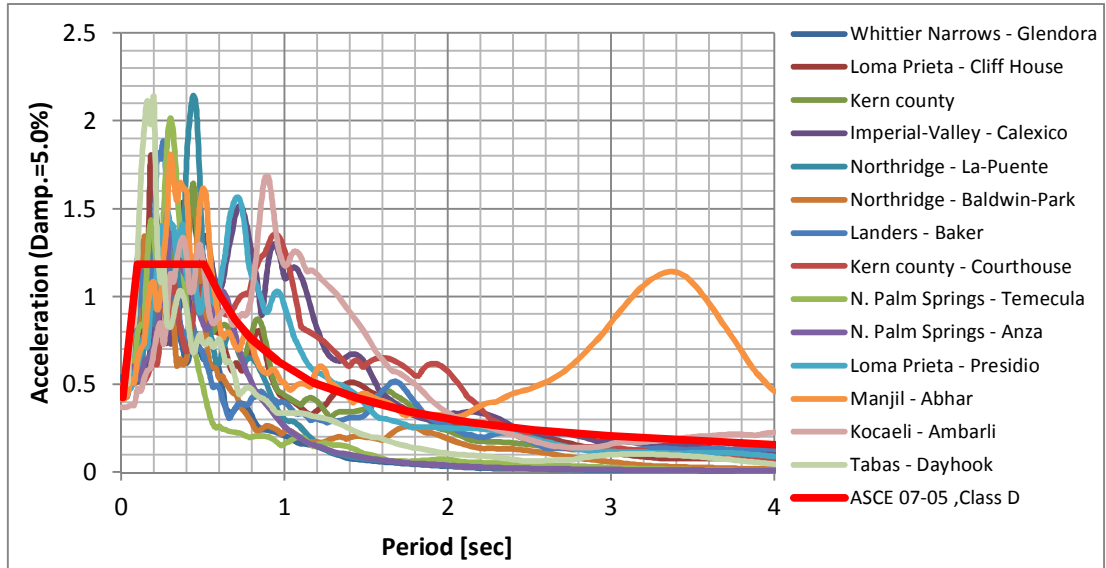


Figure 4.3. Far Faults ground motions were scaled to ASCE 7-05 standard.

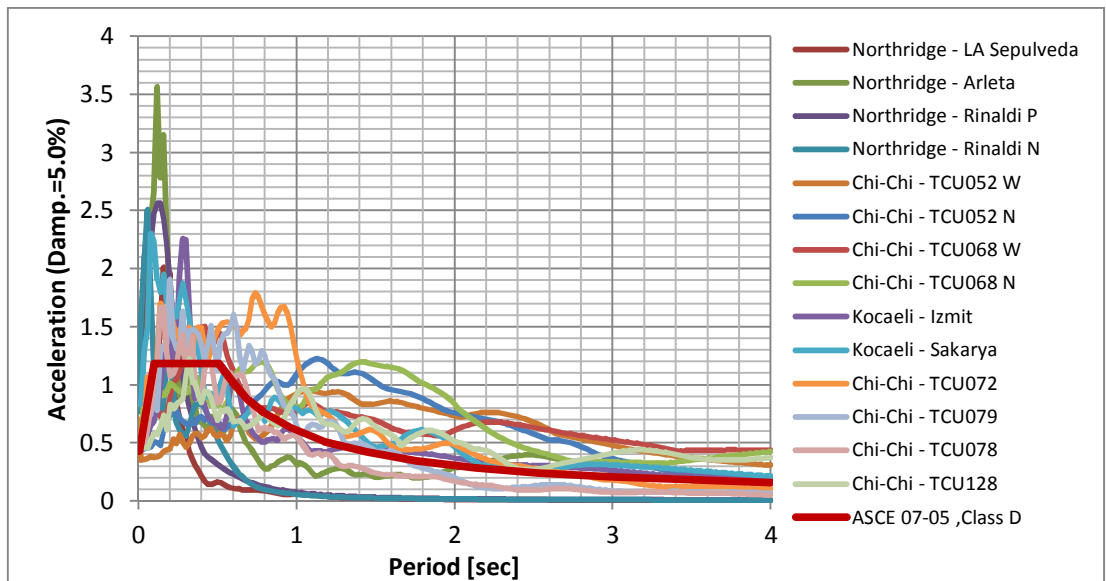


Figure 4.4. Near Faults ground motions were scaled to ASCE 7-05 standard.

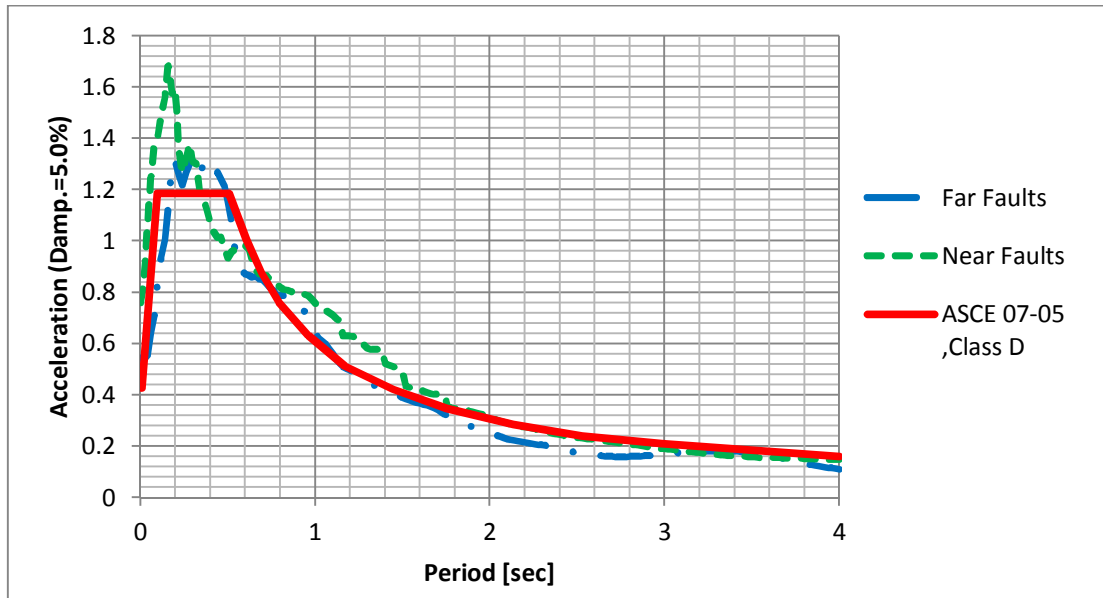


Figure 4.5. Near Faults & Far Faults ground motions compare with ASCE 7-05 standard.

## Chapter 5

### RESULTS AND DISCUSSION OF THE RESULTS

#### 5.1 Introduction

Here are the results of the analyses of building models affected by near-fault and far-fault ground motion. The records were studied using incremental dynamic analysis. The analysis comprises plotting and comparisons of seismic shear distribution, total displacement of storeys, relative displacement profile and the capacity curves (pushover).

It should be noted that each building model is studied under near-fault as well as far-fault ground motion. This resulted in 84 nonlinear time history analyses (28 records for each building model). The 1<sup>st</sup> index of seismic demand used here is inter-storey relative displacement, defined as the relative displacement between two adjacent floors divided by the height of the storey. Non-linear time history analysis results for buildings with moment frames are plotted below, with the results pertaining to maximum lateral displacement under both groups of ground motion. For these models of building, far-fault motions result in nearly uniform lateral displacement requirements with the exception of a small record in the 10-storey building which will create more displacements. Near-fault conditions produce higher requirements when compared to far-fault conditions. With near-field ground motions involving fling-step, TCU-52 creates the largest displacement in 6- and 10-storey buildings.

Based on different analyses, the presented results include total displacement profile of storey per cent, inter-storey displacement profile per cent, shear profile at storeys per cent. Moreover, the capacity curve (pushover) is presented for each building model.

## 5.2 Ground motion records

- Near-fault records accelerograms.
- Far-fault records accelerograms.

## 5.3 Results extraction

As mentioned previously, the results presented in this study include total displacement profile of storey per cent, inter-storey displacement profile percent, shear profile at storeys percent. Moreover, the capacity curve (pushover) is presented for each building model. Total displacement profile of storey per cent is obtained as follows (Eq 5.1):

$$\text{Total displacement of storey (\%)} = \frac{(\text{Total displacement of storey (m)})}{\text{Overall height of the building (m)}} \times 100$$

Overall height of 6-storey building equals to 19.2 meters, 10-storey equals to 32 meters, 15-storey equals to 48 meters. The total displacement of each storey is obtained via the analyses performed.

Inter-storey displacement profile per cent is obtained as follows (Eq 5.2):

$$\text{Inter – storey displacement (\%)} = \frac{\text{Inter – storey displacement (m)}}{\text{Total height of the storey (m)}} \times 100$$

Inter-storey displacement (m) - upstairs displacement (m) - downstairs displacement (m)

For all models, the total height of storey is 3.2 meters and displacement values of storeys are obtained via the analyses. Generally, in earthquake engineering, inter-

storey displacement is more important than the total displacement. In fact, this value shows the displacement differences between two consecutive floors which is main cause of destruction due to the earthquake. Shear profile at storeys percent is obtained as follows (Eq 5.3):

$$\text{Shear of storey (\%)} = \frac{\text{Shear of storey}}{\text{Overall weight of the building}} \times 100$$

Shear values of storeys are extracted from the analyses.

## **5.4 Analyses results**

### **5.4.1 IDA Curves**

Nonlinear Response History Analysis (NRHA) can be used for the seismic performance assessment of structures in the framework of IDA (Cornell, 2002). IDA involves repeatedly running NRHAs using a suite of ground motions scaled to different factors such that the response to each ground motion is obtained at many different intensities. Specifically, for any Engineering Demand Parameter (EDP) used to characterize structural response and Intensity Measure (IM), e.g. the 5% damped, first mode spectral acceleration  $S_a(T_1, 5\%)$ , we can generate IDA curves consisting of the EDP plotted as a function of the IM for each record.

Conventionally, the response EDP (dependent parameter) is plotted on the abscissa, and the IM (independent variable) is plotted on the ordinate. Given these IDA curves, the statistical distribution of response as a function of input can be summarized by curves that represent the 16%, 50% and 84% fractiles. Summarize the IDA curves and limit-state capacities across all records into 16%, 50% and 84% fractile by the standard deviation.

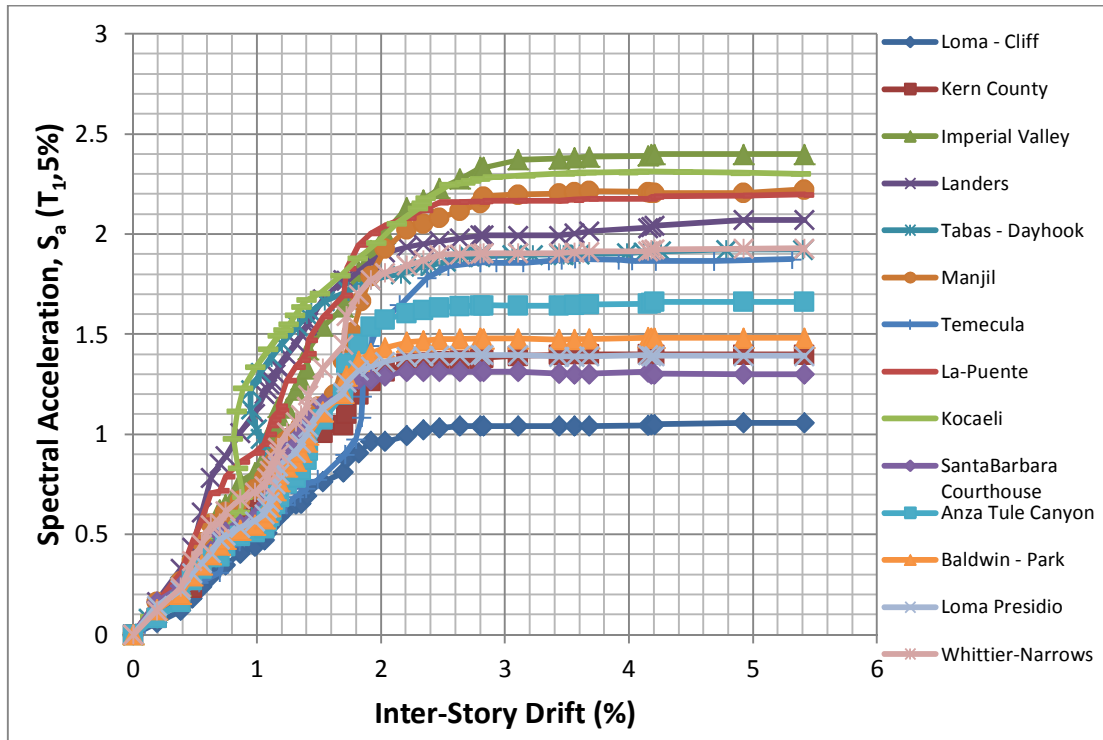


Figure 5.1. IDA curves and limit-state capacities for 6-story building: IDA curves for 14 far faults ground motions.

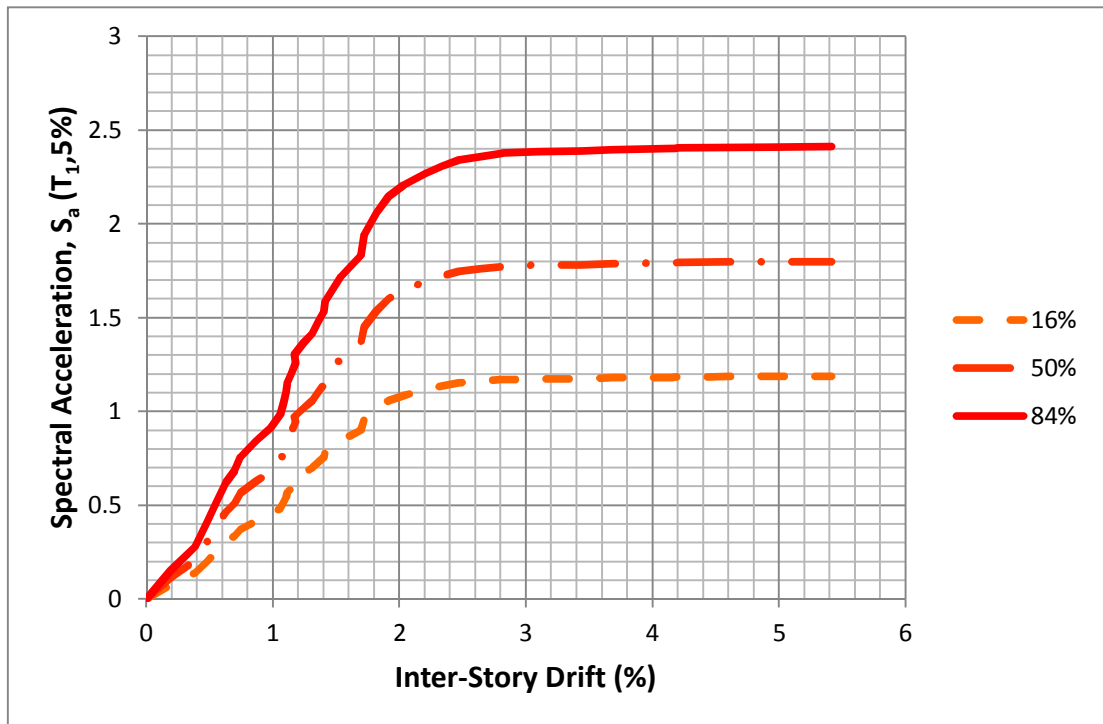


Figure 5.2. The summary of IDA curves for 6-story building (Far fault ground motions).

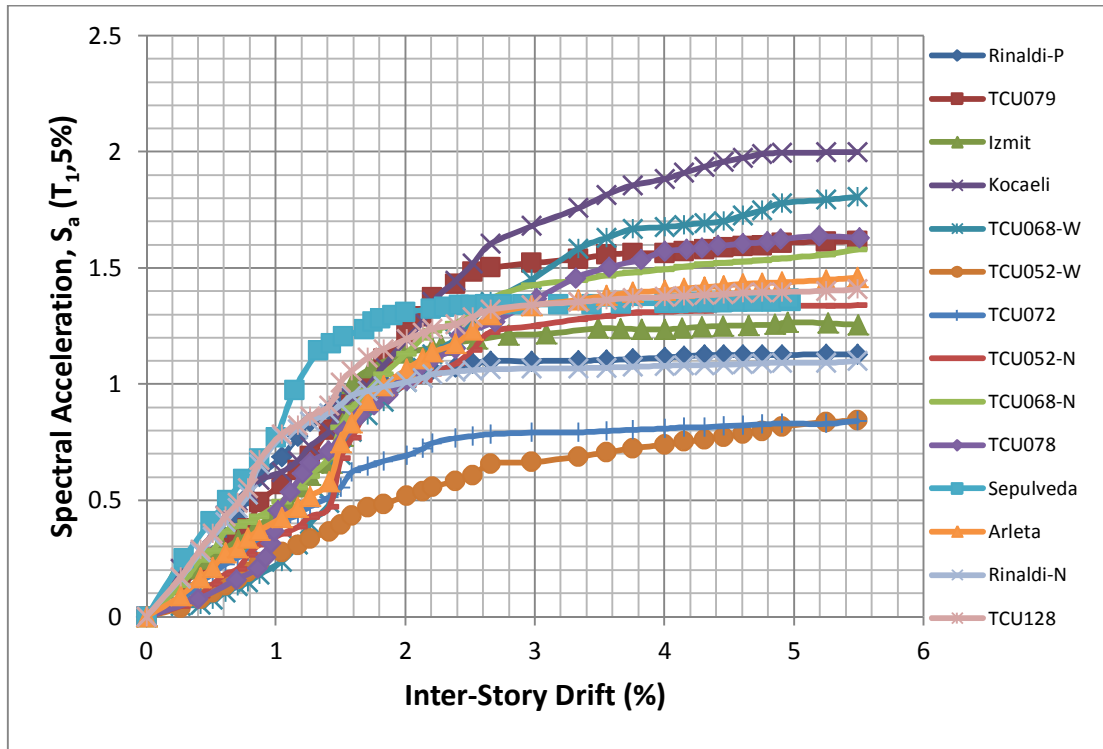


Figure 5.3. IDA curves and limit-state capacities for 6-storey building: IDA curves for 14 near faults ground motions.

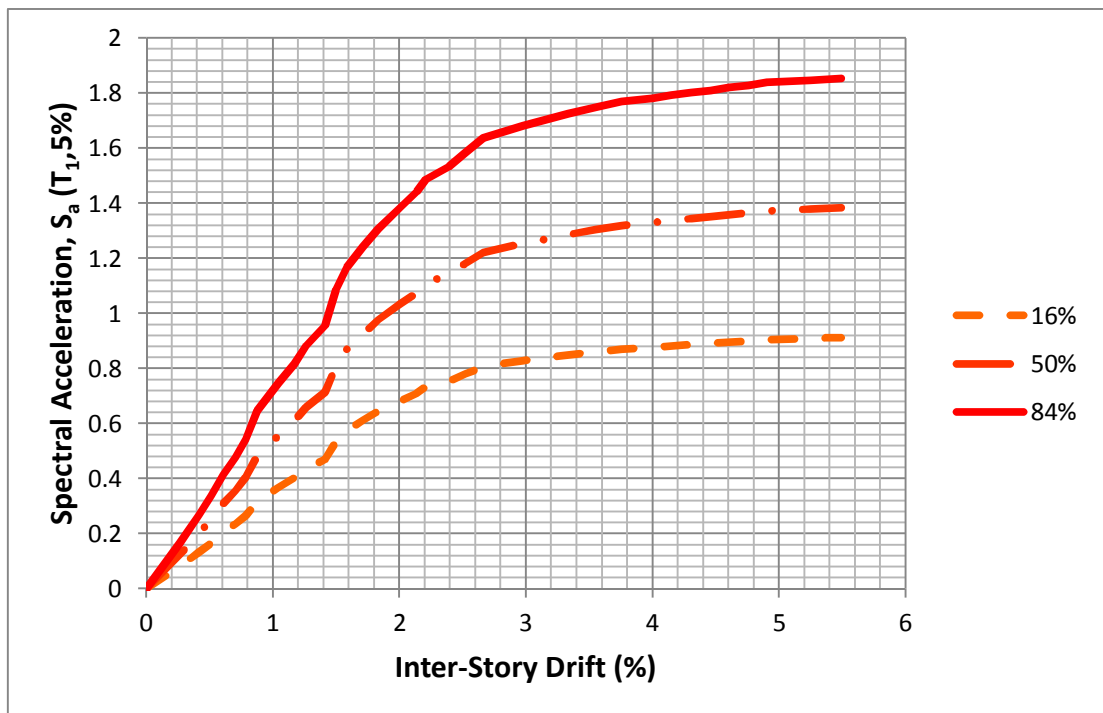


Figure 5.4. The summary of IDA curves for 6-storey building (Near fault ground motions).

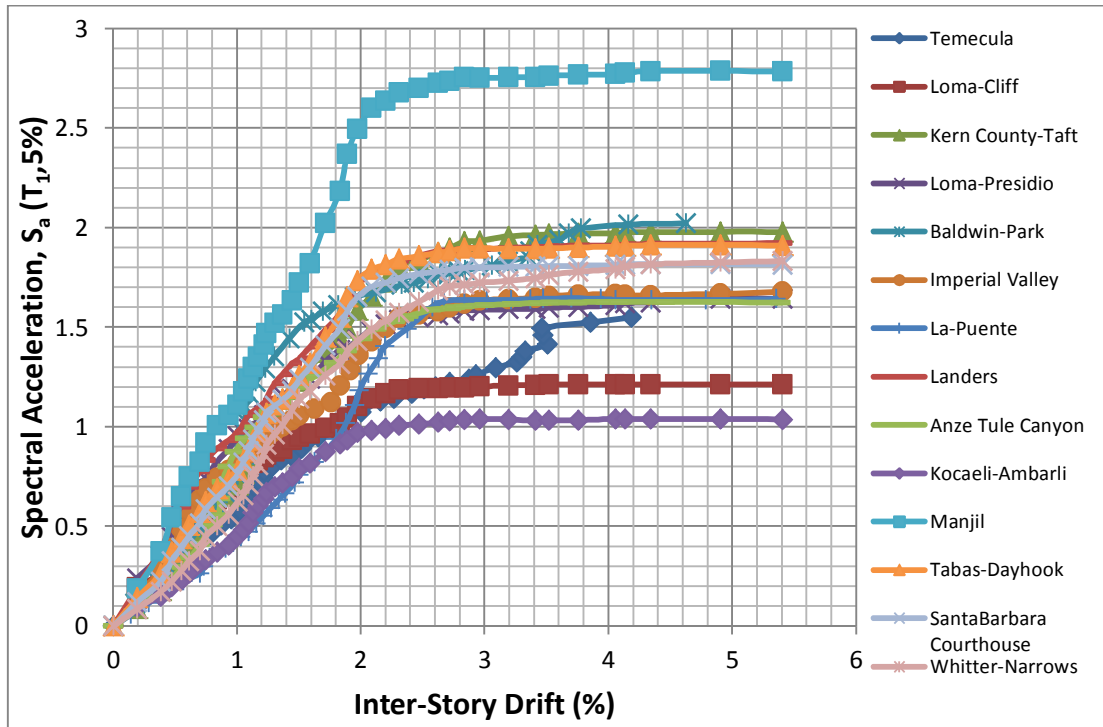


Figure 5.5. IDA curves and limit-state capacities for 10-storey building: IDA curves for 14 far faults ground motions.

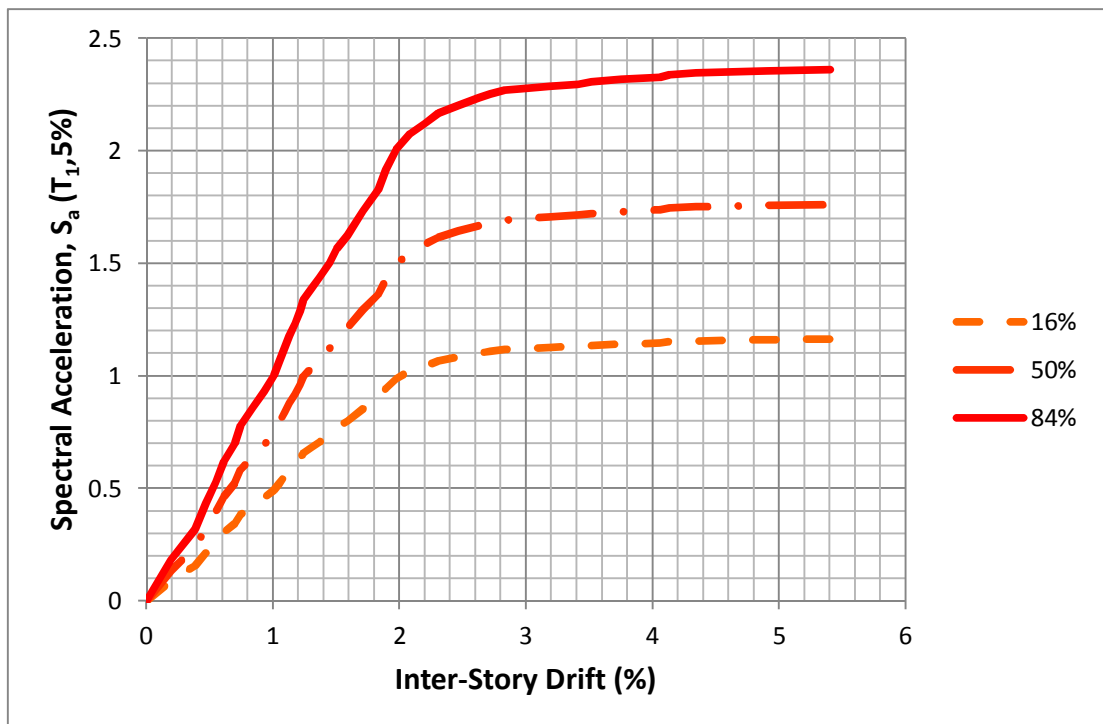


Figure 5.6. The summary of IDA curves for 10-story building (Far fault ground motions).

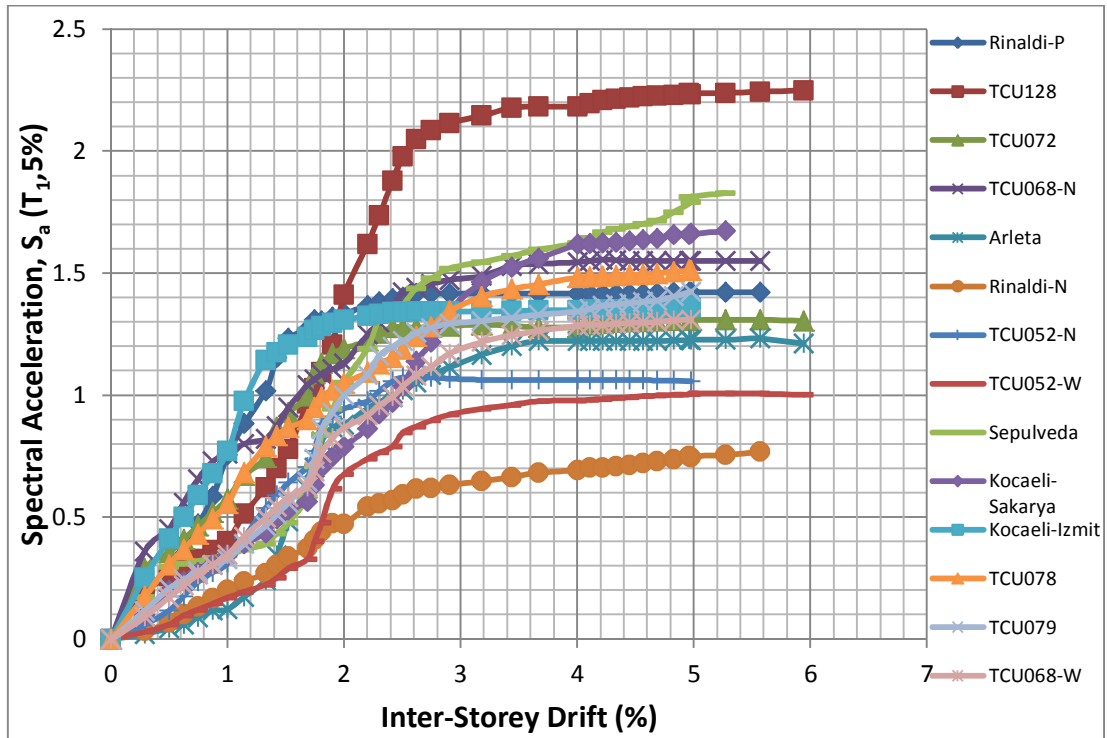


Figure 5.7. IDA curves and limit-state capacities for 10-storey building: IDA curves for 14 near faults ground motions.

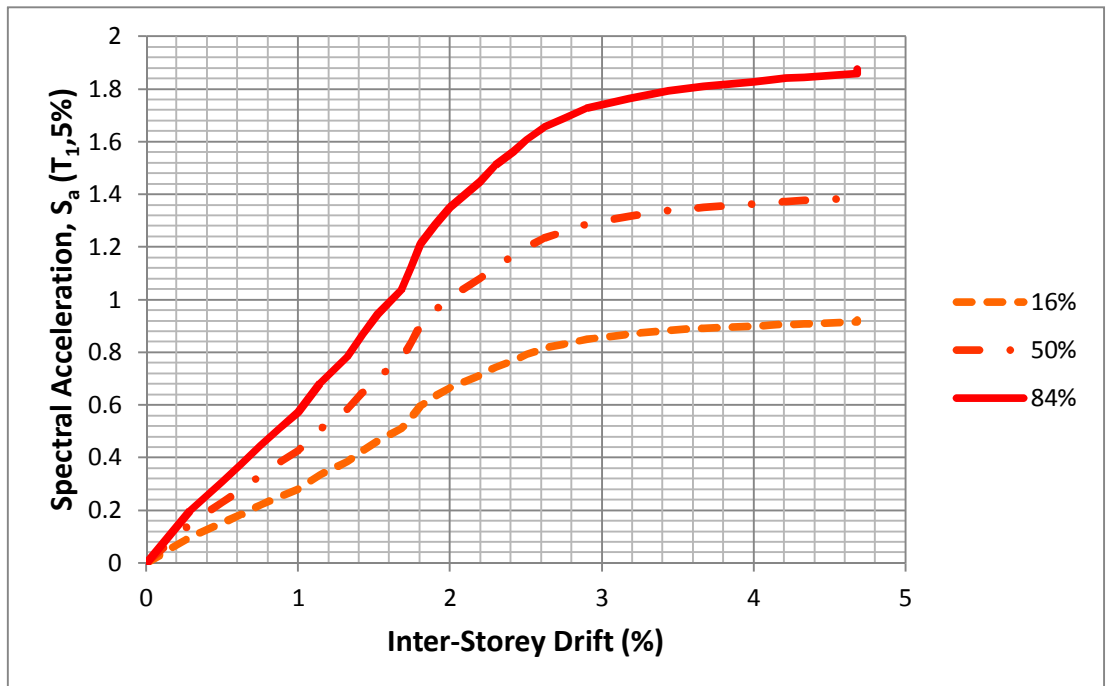


Figure 5.8. The summary of IDA curves for 10-story building (Near fault ground motions).

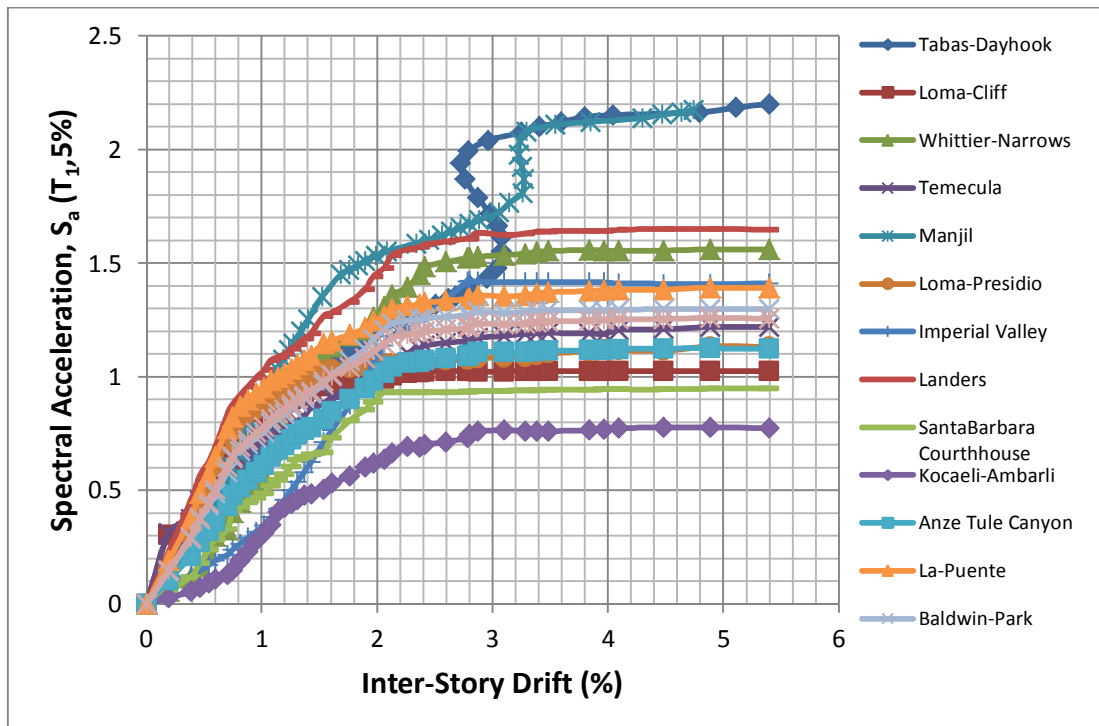


Figure 5.9. IDA curves and limit-state capacities for 15-storey building: IDA curves for 14 far faults ground motions.

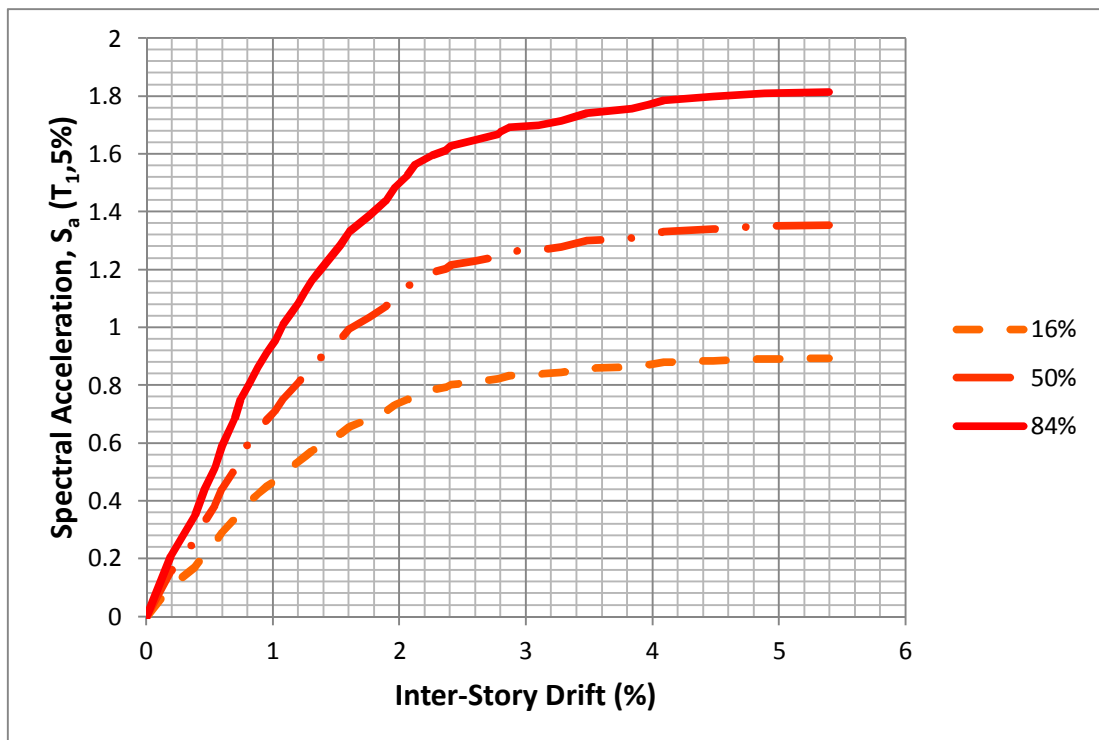


Figure 5.10. The summary of IDA curves for 15-storey building (Far fault ground motions).

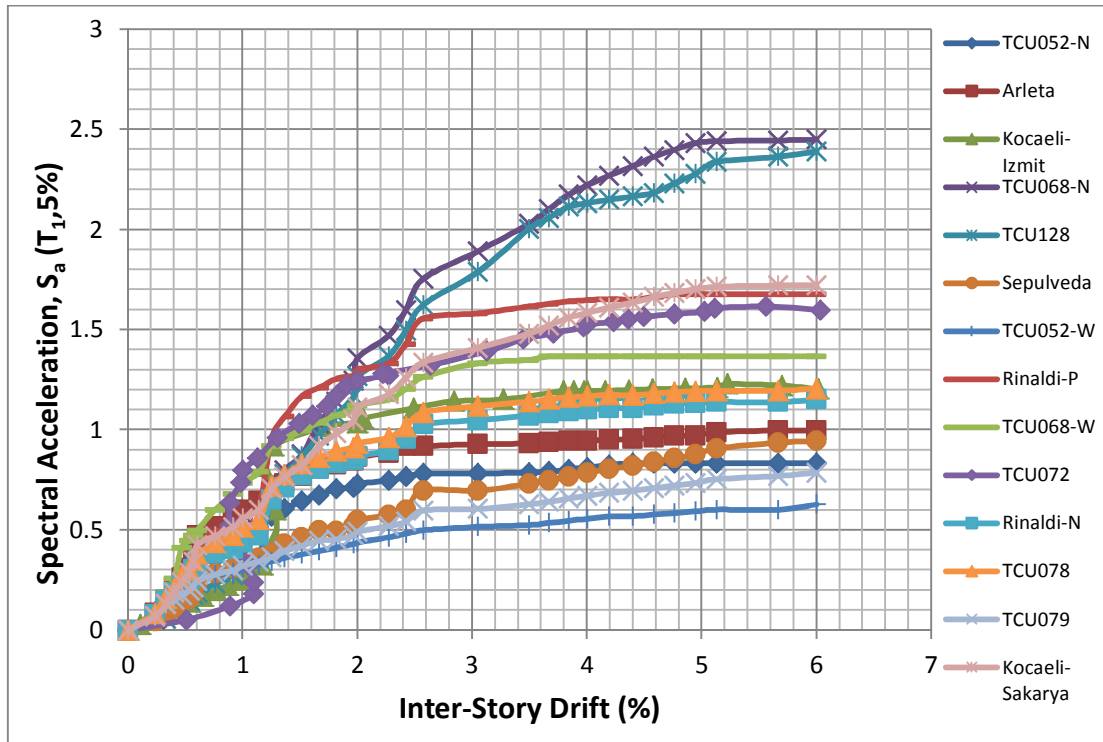


Figure 5.11. IDA curves and limit-state capacities for 15-storey building: IDA curves for 14 near faults ground motions.

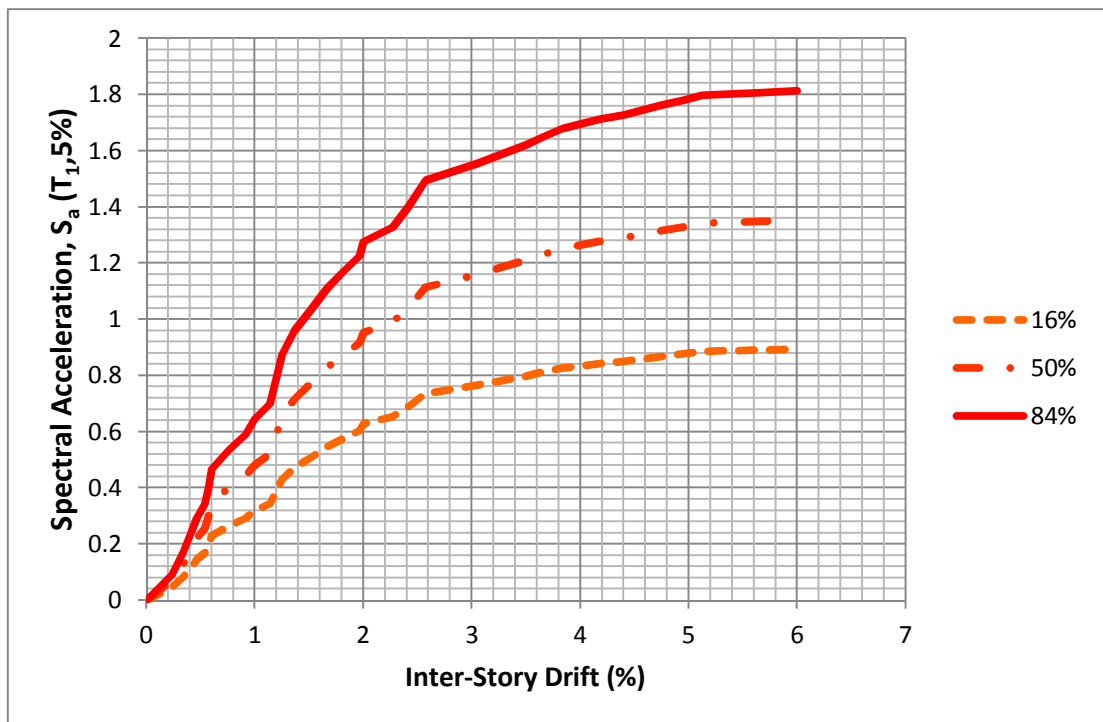


Figure 5.12. The summary of IDA curves for 15-storey building (Near fault ground motions).

#### **5.4.2 Storey model, far-fault & near-fault**

According to the Non-Linear Incremental Dynamic analysis (IDA) for far and near fault zone the below results for 6-story, 10-story and 15-story have been revealed respectively.

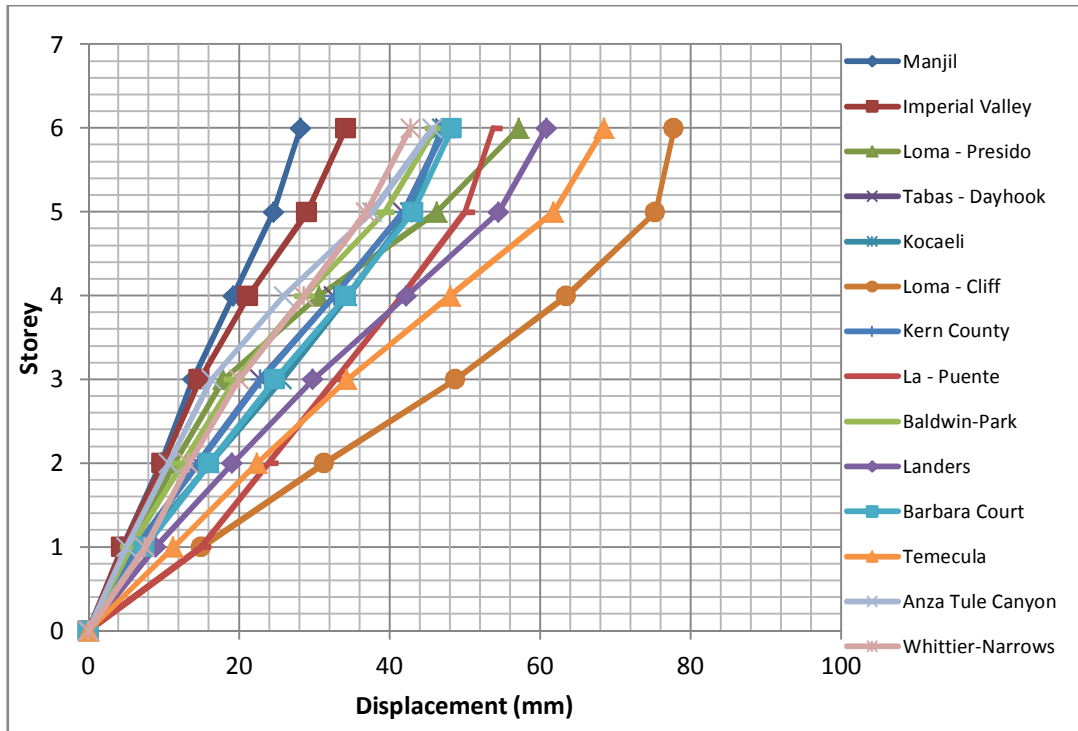


Figure 5.13. Total displacement profile of 6-storey for far faults

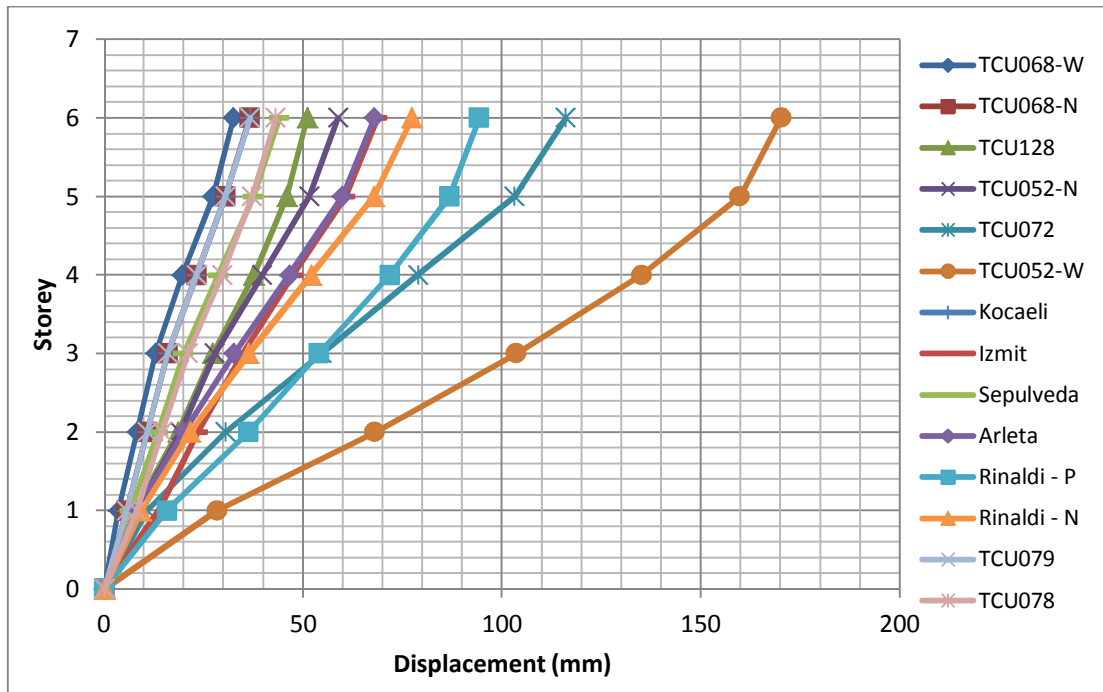


Figure 5.14. Total displacement profile of 6-storey for near faults

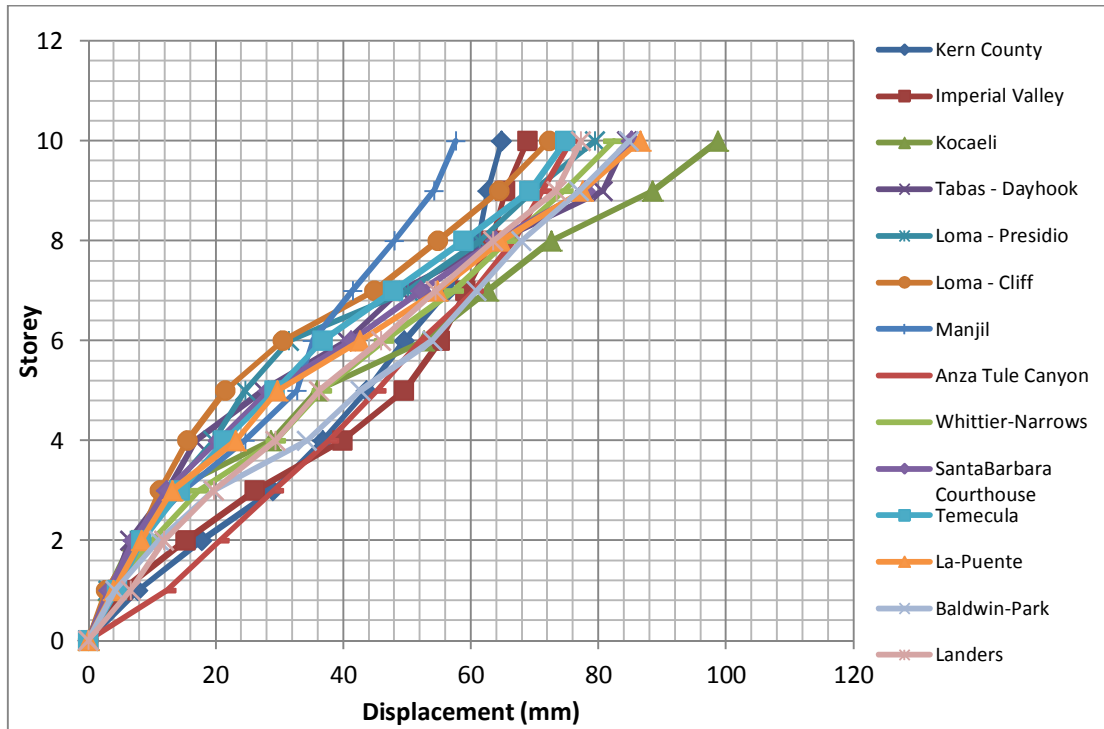


Figure 5.15. Total displacement profile of 10-storey for far faults

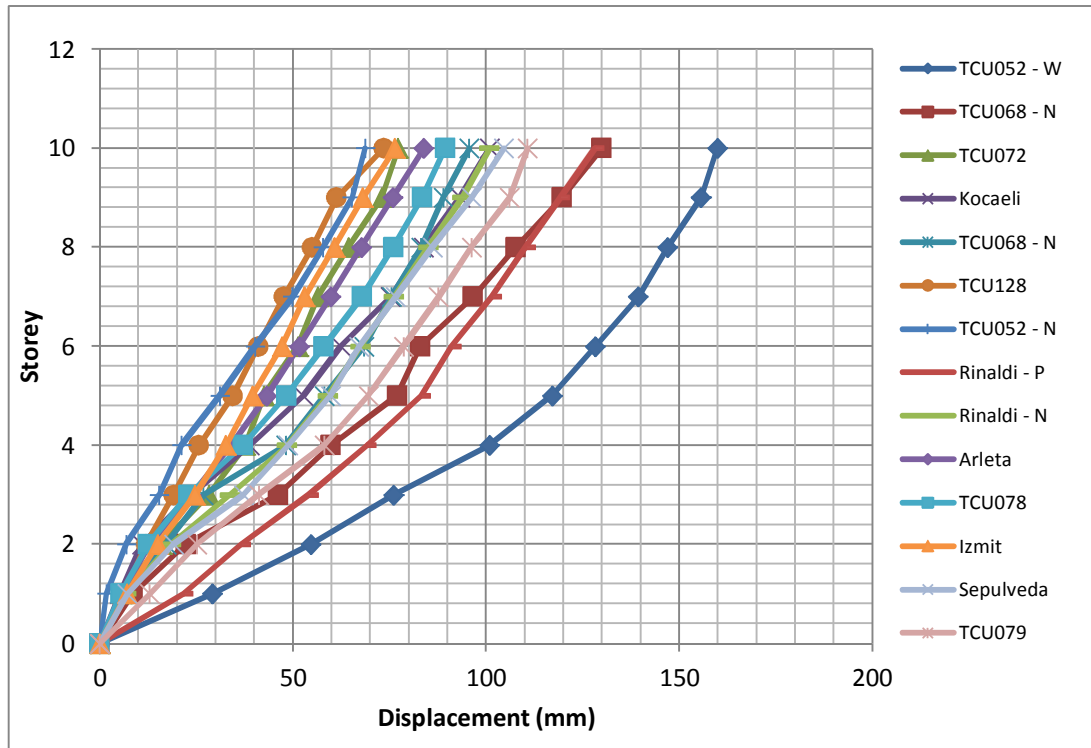


Figure 5.16. Total displacement profile of 10-storey for near faults

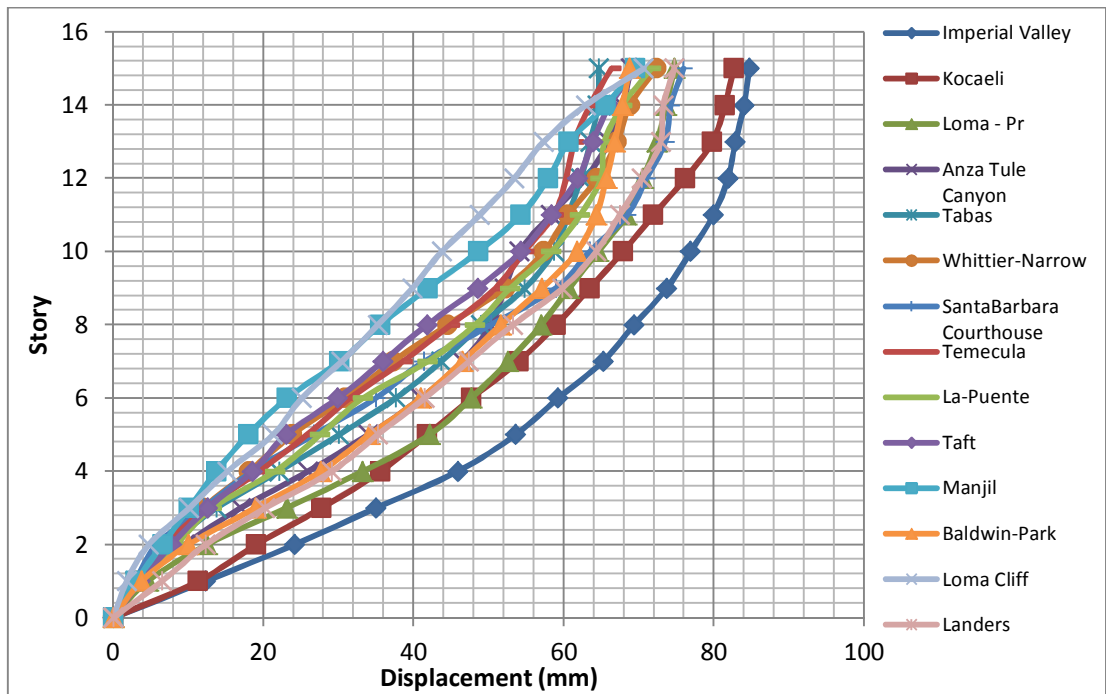


Figure 5.17. Total displacement profile of 15-storey for far faults

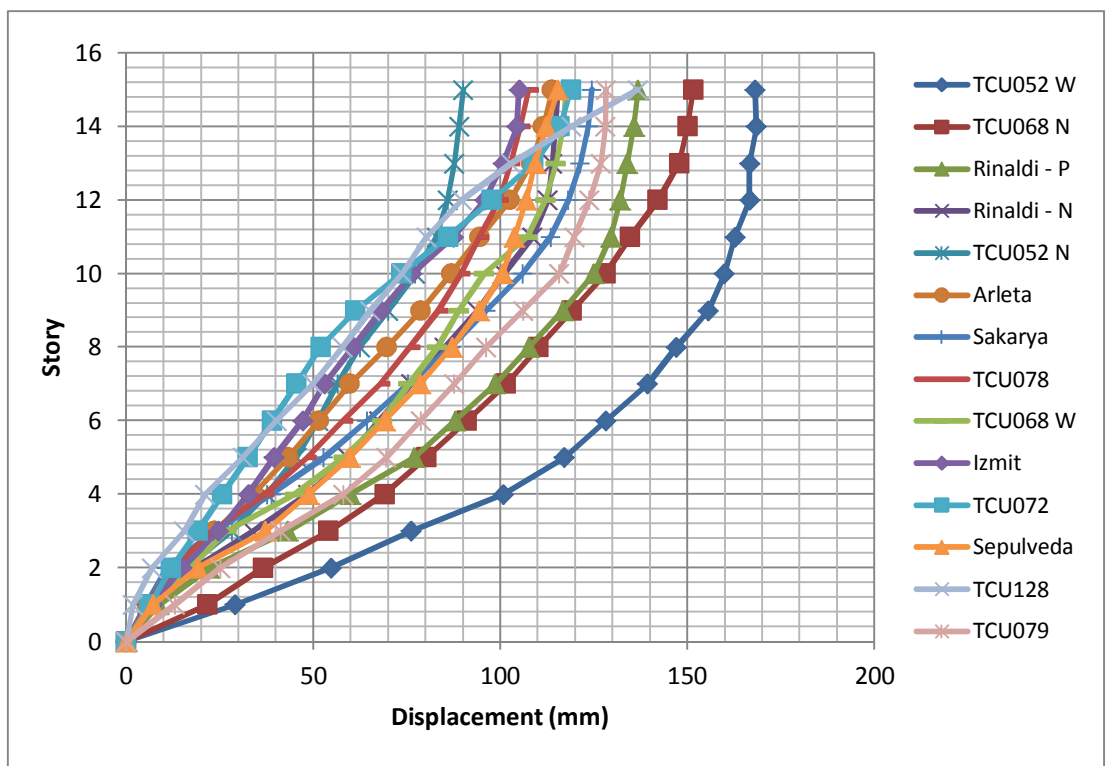


Figure 5.18. Total displacement profile of 15-storey for near faults

By comparing the mean values of the maximum storey displacement under near- and far-field records, it can be seen that in 6-storey building, a maximum storey displacement of 148.28 mm is produced, being 90 percent more than 78.01 mm due to far-field records. In 10-storey building, this value equals to 160.04 mm, which is 67 percent more than 96.10 mm resulted from far-field records. In 15-storey building, this value equals to 169 mm, which is 90 percent more than 88.5 mm resulted from far-field records.

Table 5.1. Comparing the mean values of the maximum displacement under near- and far-field ground motion records (mm)

Building	Near Fault Filing Step	Far Fault	NF Filing FF
6-Storey	148.28	78.01	1.90
10-Storey	160.04	96.10	1.67
15-Storey	169.00	88.50	1.90

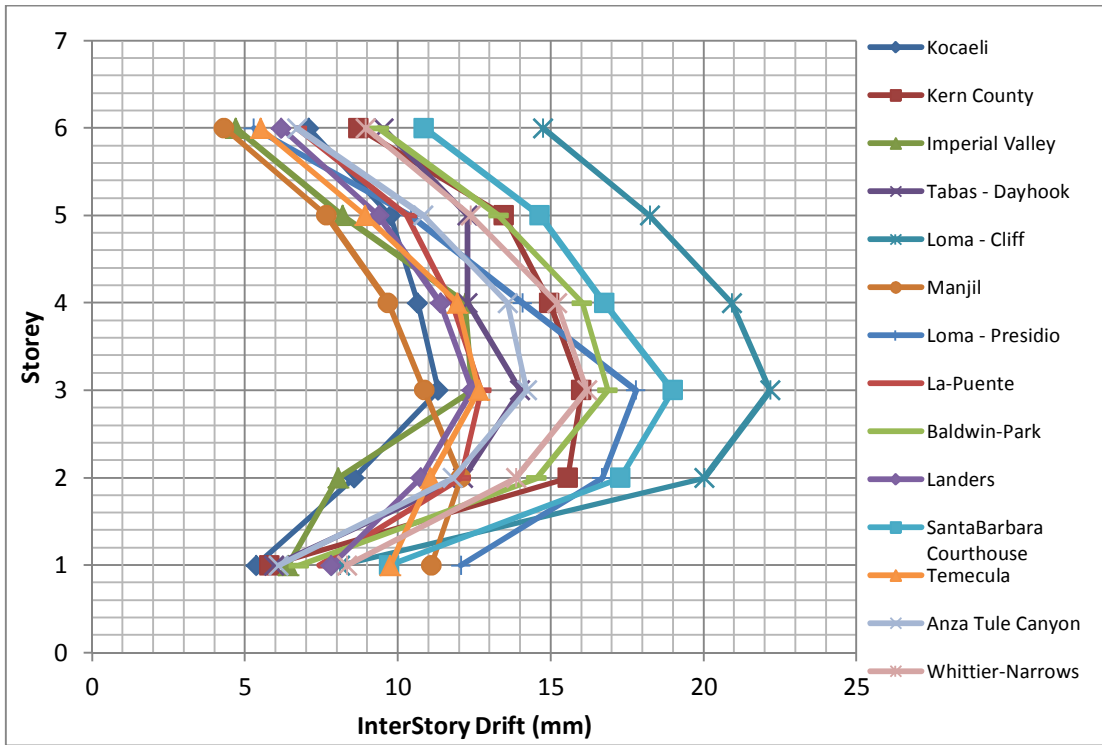


Figure 5.19. Inter-Story Drift profile of 6-storey for far faults

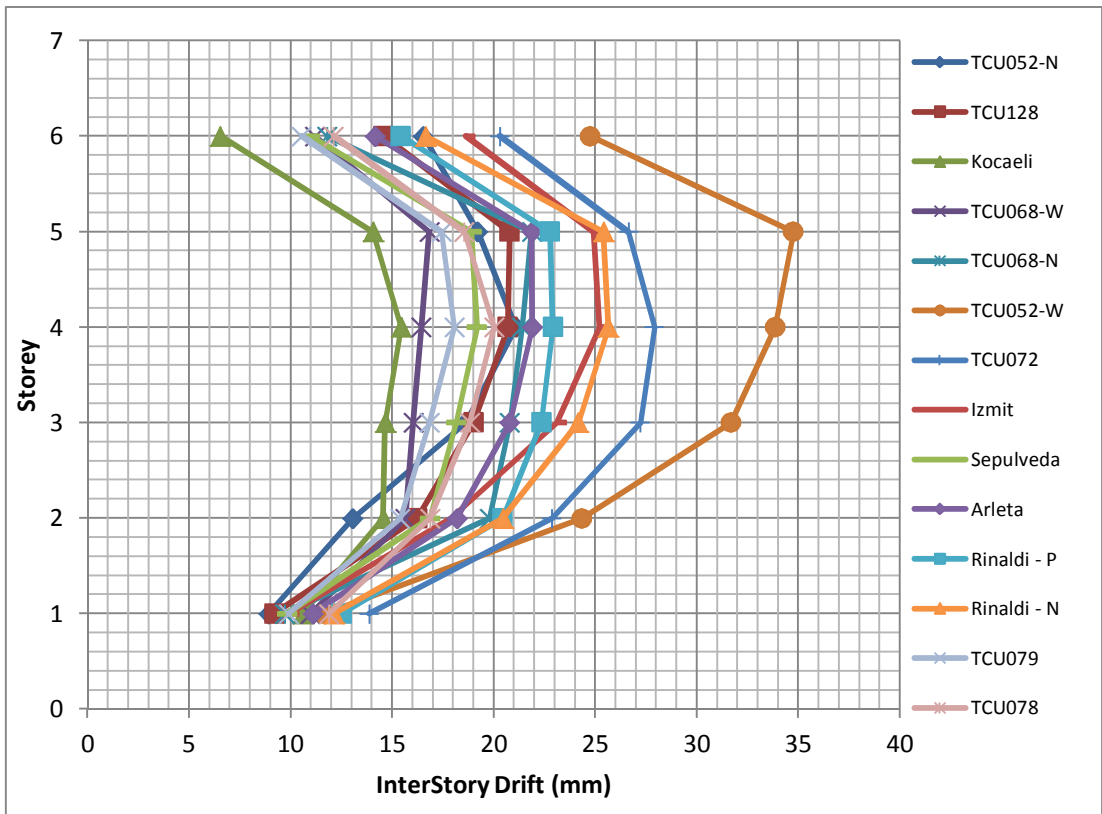


Figure 5.20. Inter-Story Drift profile of 6-storey for near faults

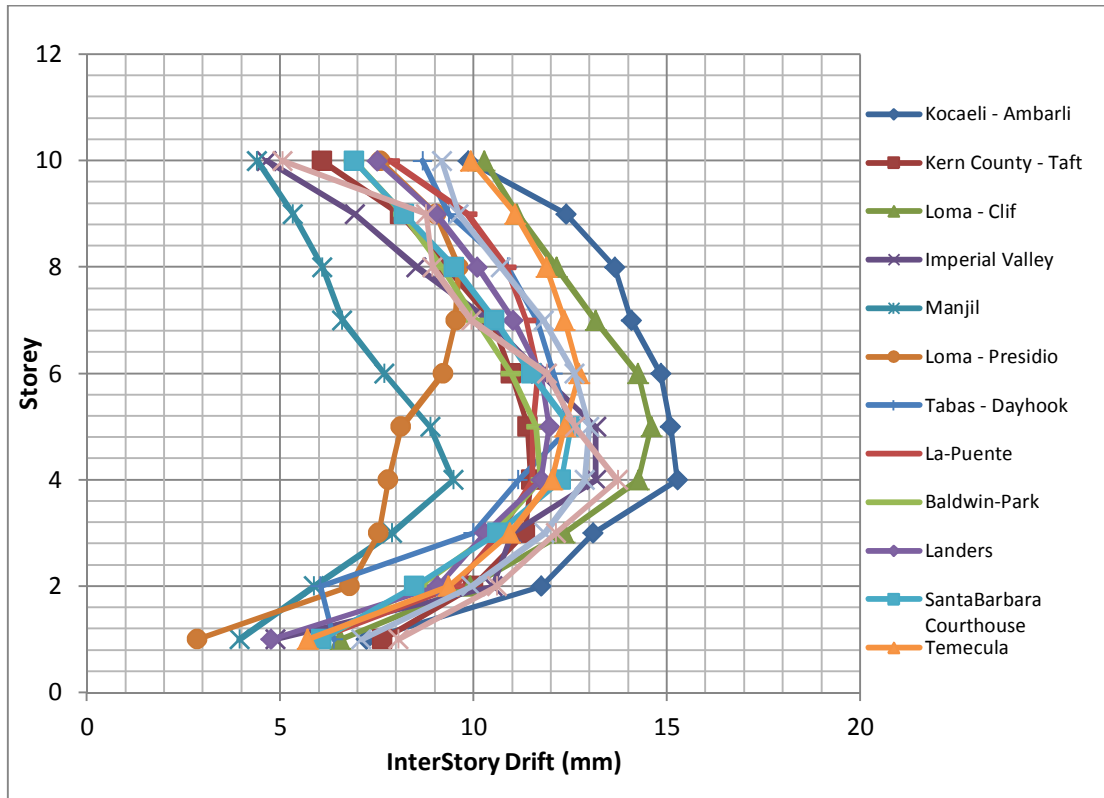


Figure 5.21. Inter-Story Drift profile of 10-storey for far faults

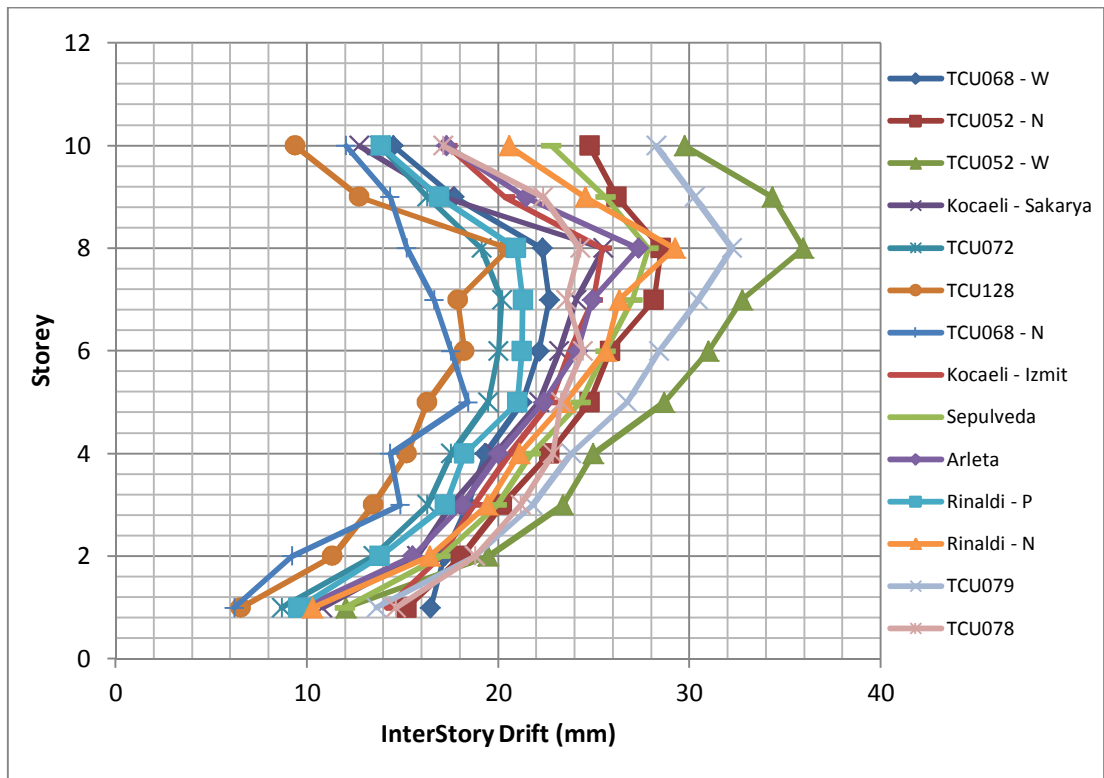


Figure 5.22. Inter-Story Drift profile of 10-storey for near faults

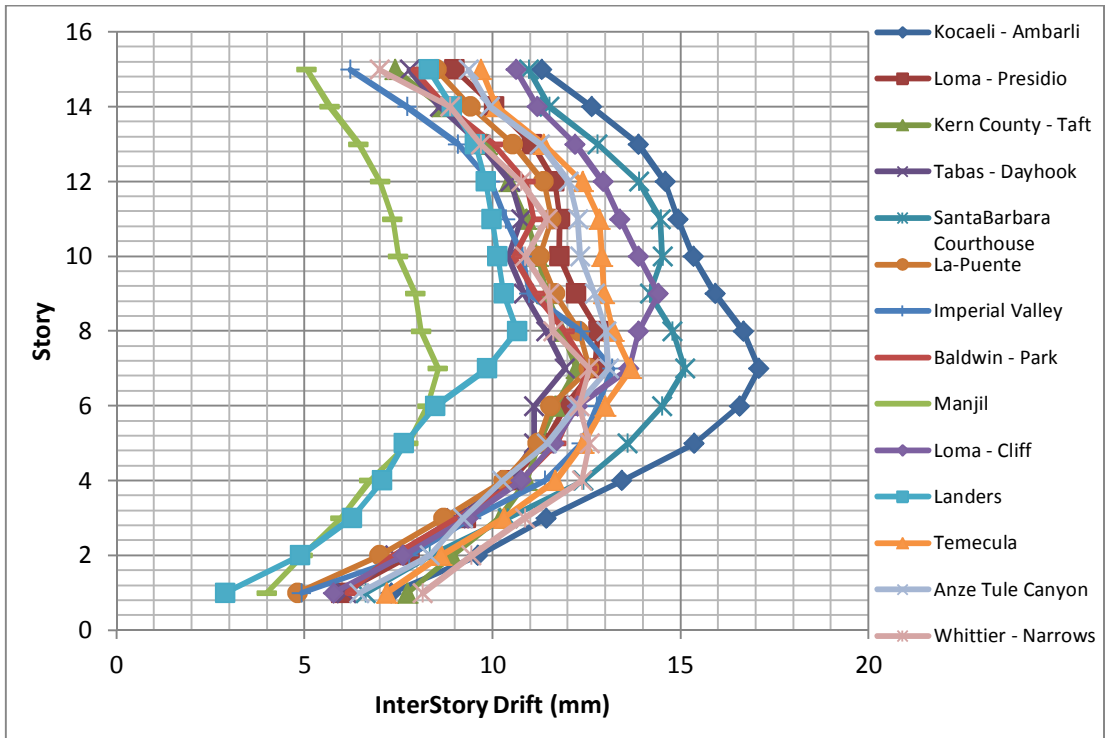


Figure 5.23. Inter-Story Drift profile of 15-storey for far faults

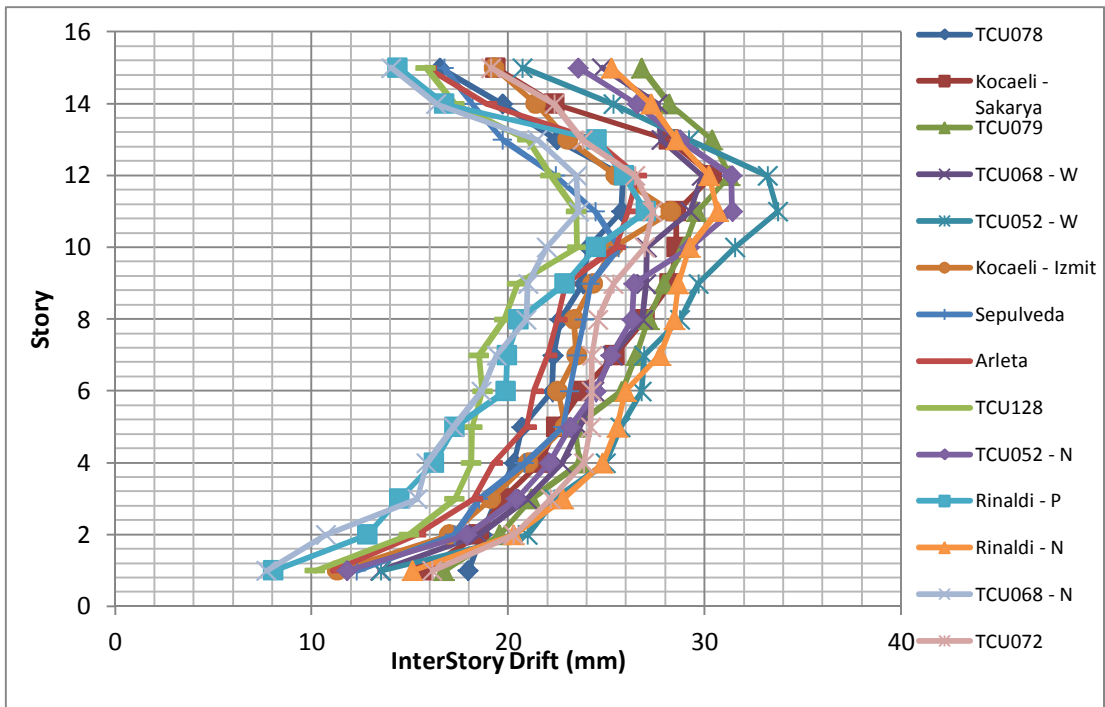


Figure 5.24. Inter-Story Drift profile of 15-storey for near faults

By comparing the mean values of the maximum inter-storey drift under near-field and far-field records, it can be seen that for 6-storey building, a maximum inter-storey drift of 22.40 mm is produced, being 50 percent more than 15.01 mm due to far-field records. In 10-storey building, a maximum inter-storey drift equals to 24.06 mm, which is 98 percent more than 12.10 mm resulted from far-field records. In 15-storey building, a maximum inter-storey drift equals to 32.16 mm, which is 87 percent more than 17.12 mm resulted from far-field records. The results show near-field records introduce significant demands on the upper floors of the structure. Many of near-field records have been affected significantly by higher modes, shifting the requirements from the lower storeys to upper ones.

Table 5.2. Comparing the mean values of the maximum inter-story drift under near- and far-field ground motion records (mm)

Building	Near Fault Filing Step	Far Fault	NF Filing FF
6-Storey	22.40	15.01	1.50
10-Storey	24.06	12.10	1.98
15-Storey	32.16	17.12	1.87

Although expected the higher modes effects on the response of high-rise buildings, but 6-storey building responses showed the non-deniable role of higher modes on the responses of low-rise buildings. In order to determine the effect of higher modes, it is necessary to examine both velocity and acceleration spectra of ground motions. Fig. 5.25 and Fig.5.26; shows the spectral velocity of some critical records, producing the most requirements in buildings. It should be noted that the modal periods in a nonlinear system are continuously changing but the so-called higher-mode periods start changing while entering the inelastic range. Modal periods in the elastic range are shown in dotted lines at Fig.5.25 and Fig.5.25. Gradually all of these lines shift to

the right, while the members are yielding. The buildings' responses were checked again in order to find a relation between the information of spectral demand and the observed behaviour of the building.

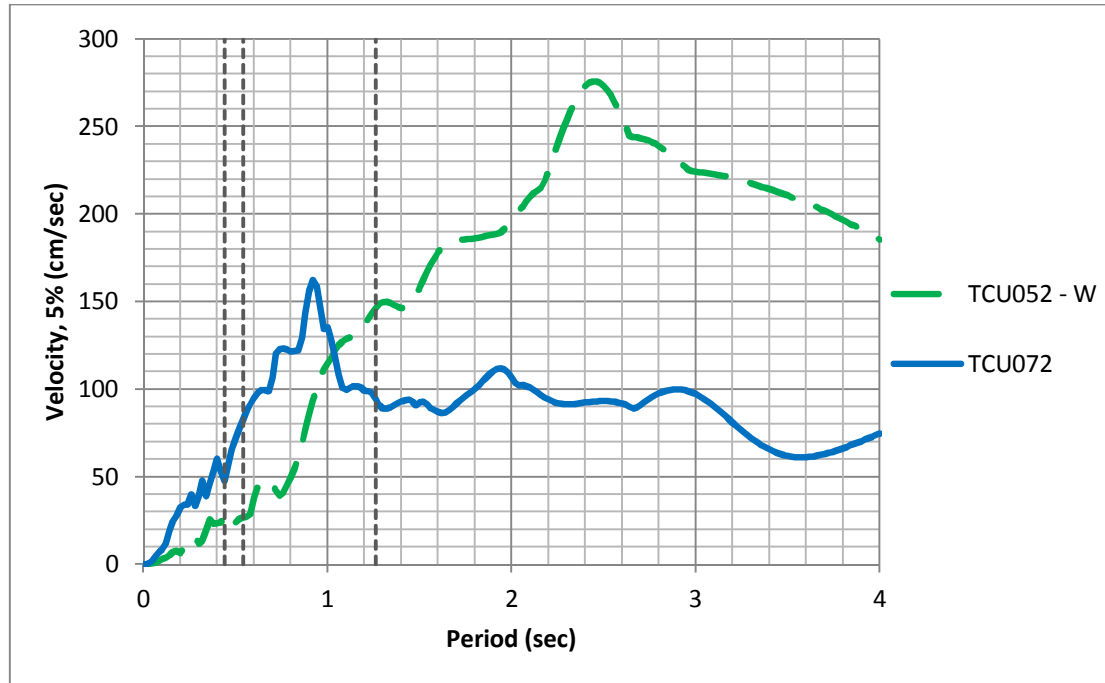


Figure 5.25. Spectral velocity of the selected ground motion records for 6-story

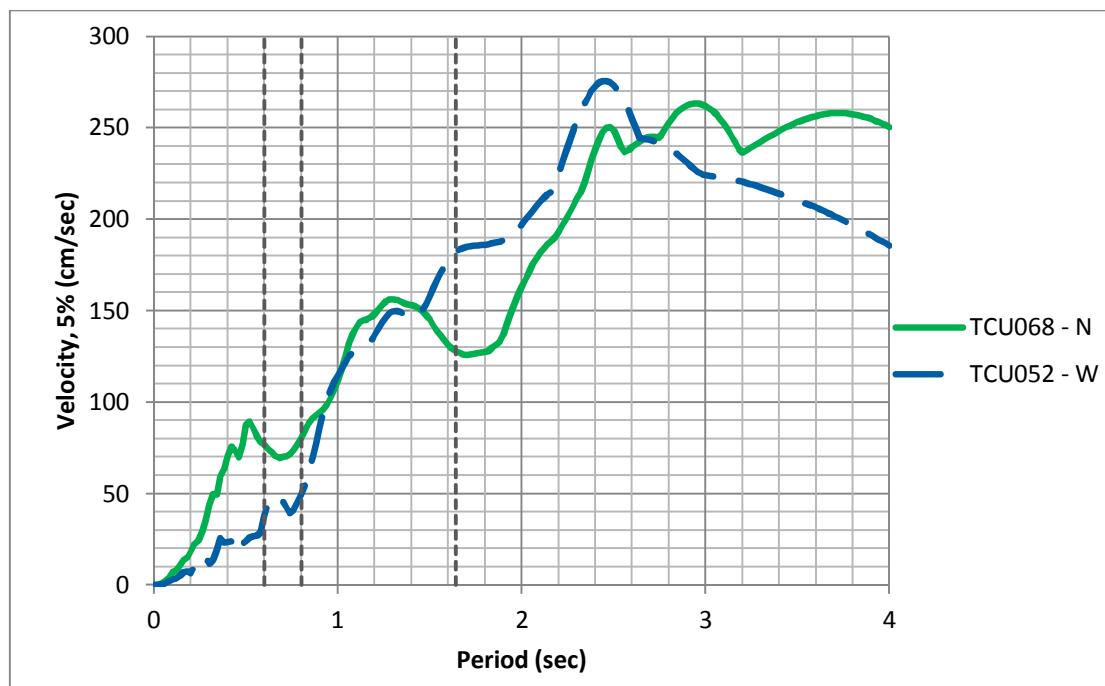


Figure 5.26. Spectral velocity of the selected ground motion records for 10-story

In the records TCU-52 and TCU-68, the structure was most-affected by higher modes, resulting in an increased requirement in the intermediate and upper floors. In the record TCU-52, spectral velocities in modes II and III were significantly more than the first mode's. For this record, the first mode response of velocity spectra was quite clearly observed. Similarly, by looking at the velocity spectra of TCU-52 and TCU-68, higher-mode responses of 10-story building can be observed. In summary we can say that, for near-fault records, the average of maximum requirements and dispersion of maximum values of the buildings are higher than those for far-fault records. In general, the effects of higher modes in the records involving fling-step were most evident.

## **5.5 Discussion**

In this thesis, fling-steps were studied by evaluation of responses to near-fault ground motions involving fling-step. The results of this study showed that in compare to far-fault records, near-fault ones involving fling-step cause more damage to the structures. The results showed that a careful and simultaneous examination of the spectrum of acceleration and velocity, both together, can help the engineers to assess the damage potential of near-field records. The variable maximum demand which a storey has from one record to the next is the most important observation from the evaluation of non-linear time history of reinforced concrete structures. In this study, the shear distribution at storeys, displacement profile of storeys, inter-storey relative displacement profile and the demand curve for structures are compared together. According to presented results, in the studied structures, the building shear base and deformation increases with higher number of floors. The reason is that, in the same conditions, the higher the number of floors, the lower the structural stiffness. As a result, the natural period of the structure increases.

Inter-storey relative displacement is one of the important factors affecting the failure rate in the structure. Therefore, it is a good measure for assessing the performance of seismic resistance especially if near-fault ground motions are likely to happen. Near-fault ground motions usually have quick blow with high period which may be identical or near to the period of building. In such cases, the building may be exposed to severe deformation. The results of the analyses show this approach. In fact, under the same conditions, further displacements may occur due to near-fault earthquakes than those of far-fault ones. This is an important note, especially in high-rise buildings. Pulse-like near-fault earthquakes occurring due to directivity are a particular kind of earthquakes widely studied. According to the existing pulse in velocity time history, this type of earthquake is described in the normal direction to the fault line and usually occurs in an area located a short distance to the fault. Understanding the effects of this earthquake on structures is very important because it has been experienced that the damage caused by is so much. Period ( $T_p$ ) along with velocity pulse is one of the main characteristics of pulse-like earthquakes. Based on the researches,  $T_p$  can be considered a good approximation of the period in which the velocity response spectrum reaches its maximum value.

There are two approaches on the effects of near-field ground motions on structures. First, in long periods, the ground motions normal to fault line have greater spectrum values comparing to parallel motion to the fault line. Motions parallel and normal to the fault lines are more or less distinct. In addition, the maximum displacement for the normal to the fault component occurs at different time than that of parallel to the fault component. Thus the vector sum of their maximums is not possible. Second, in the near-field earthquakes, the structures are severely shaken due to the long pulses

exist. These pulses can cause a large displacement in the structure which has periods close to the pulses’.

The modelling results indicate that for the two earthquakes with nearly identical conditions, more displacement values are obtained in near-fault record. Overall and relative displacement increases along with the building height. Nonlinear behaviour in taller buildings is more important and nonlinear range is met in less percentile values.

## Chapter 6

### CONCLUSION AND RECOMMENDATIONS FOR FURTHER RESEARCH

#### 6.1 Conclusion

The damage and failure of engineering structures observed during recent earthquakes show the damage potential of existing buildings to near-fault ground motions but there are still considerable unknowns about the consequences of the near-fault record on the response of common building structures. In existing guidelines, the effects of long-period pulses are not considered suitably in the design process. The simple methods using magnification of design spectra to determine the inelastic demands, do not estimate acceptable solutions for near-field records. Therefore, the aim of this research is to acquire new information about the responses of moment frames to near-fault ground motions and the extent of differences existing in compare to those of far-fault ones.

As noted, the present study was to evaluate the seismic structural performance of reinforced concrete buildings under near- and far-fault ground motion records based on incremental dynamic analysis methods. For this purpose, a 6-storey building as a low-rise and a 10 and 15-storey building as a mid-rise building have been studied. Numerical modelling carried out in this thesis showed that the reinforced concrete buildings are under large deformation requirements during the presence of velocity pulses in velocity time history. This requires a considerable amount of energy to be

wasted in one or more cycles of Structural Plastics Limited. This requirement makes the structures to meet with limited ductility capacity. In contrast, the far-fault motions enter the input energy into the system gradually. Although, on average, deformation demands are less than those in the near-fault records, but structural systems are subjected to more plastic cycles.

Therefore, the cumulative effects of far-fault records are minor. It has been recently known that the near-fault motions involving forward-directivity have further damage effects but the consequences of displacements due to recoil stroke (fling-step) are not well known.

## 6.2 Suggestions for Further Research

- The proposed method was evaluated for a particular building system. More studies for other concrete and steel building systems are recommended.
- The proposed method has only been evaluated on regular buildings. For more comprehensive review, it is recommended to study on structures with irregularities in the plans due to misalignment of centre of mass and centre of stiffness and geometric asymmetry.
- As for the widespread application of irregularities in structures at height, for more comprehensive review, it is recommended to be the goal of future research
- Due to the existing complexity, further research is required to achieve more comprehensive information about the effects of near-fault ground motions.
- For future research, the incremental dynamic analysis may be compared with other methods of dynamic analysis to assess their performances.

## REFERENCES

- Abrahamson, N.A., ( 2000), “Near-fault ground motions from the 1999 Chi-Chi earthquake”, Proceedings of the US-Japan Workshop on the Effects of Near-Field Earthquake Shaking, San Francisco, California, pp. 11- 13.
- ACI. Building code Requirements for structural concrete with commentary. ACI 318. American Concrete Institute; 2008.
- American Society of Civil Engineers (ASCE). Minimum design loads for buildings and other structures. ASCE Standard No. ASCE/SEI 7-05; 2006.
- Baker, J.W., and Cornell, C. A. (2006). “Spectral shape, epsilon and record selection.” *Earthquake Eng. Struct. Dyn.*, 35, 1077–1095.
- Curt B. Haselton, "Evaluation of Ground Motion Selection and Modification Methods: Predicting Median Interstory Drift Response of Buildings", PEER Report 2009/01, Pacific Earthquake Engineering Research Center.
- Dolšek, M., and Fajfar, P. (2005). “Simplified non-linear seismic analysis of infilled reinforced concrete frames.” *Earthquake Eng. Struct. Dyn.*, 34(1), 49–66.
- Hall, J.F., Heaton, T.H., Halling, M.W. and Wald, D.J., (1995), “Near source ground motion and its effects on flexible buildings”. *Earthquake Spectra*, 11(4): 569-605.

- Han, S. W., and Chopra, A. K. (2006). "Approximate incremental dynamic analysis using the modal pushover analysis procedure." *Earthquake Eng. Struct. Dyn.*, 35, 1853–1873.
- Heaton, T. H., Hall, J. F., Wald, D. J., and Halling, M. W., (1995), "Response of high-rise and base-isolated buildings to a hypothetical MW 7.0 blind thrust earthquake". *Science*, 267: 206–211.
- Iervolino, I., and Cornell, C. A. (2005). "Record selection for nonlinear seismic analysis of structures", *Earthquake Spectra*, 21(3), 685–713.
- Kalkan, E., and Kunnath, S.K., (2006), "Effects of fling step and forward directivity on seismic response of buildings", *Earthquake Spectra*, 22(2): 376–390.
- Liao, K.-W., Wen, Y.-K., and Foutch, D. A. (2007). "Evaluation of 3D steel moment frames under earthquake excitations. I: Modeling." *J. Struct. Eng.*, 133(3), 462–470.
- Luco, N., and Bazzurro, P. (2007). "Does amplitude scaling of ground motion records result in biased nonlinear structural drift responses?" *Earthquake Eng. Struct. Dyn.*, 36, 1813–1835.
- Mavroeidis, G.P. and Papageorgiou, A.S., (2002), "Near source strong ground motion: characteristics and design issues", *Seventh U.S. National Conference on Earthquake Engineering (7NCEE)*, Boston, MA, July 21-25.

Mortezaei, A., Ronagh, H.R., Kheyroddin, A., Ghodrati Amiri, G., (2009). “Effectiveness of modified pushover analysis procedure for the estimation of seismic demands of buildings subjected to near-fault earthquakes having forward directivity”, *The Structural Design of Tall and Special Buildings*. Published Online: Oct 21 8:58AM. DOI: 10.1002/tal.

PEER (Pacific Earthquake Engineering Research Center) Strong Motion Database, University of California, Berkeley, <http://peer.berkeley.edu/>.

Shome, N., Cornell, C. A., Bazzurro, P., and Carballo, E. (1998). “Earthquakes, records, and nonlinear responses.” *Earthquake Spectra*, 14(3), 469–500.

Somerville, P., (2000), “Characterization of near field ground motions”, U.S.-Japan Workshop: Effects of Near-Field Earthquake Shaking, San Francisco, March 20&21.

Tagawa, H., MacRae, G., and Lowes, L. (2008). “Probabilistic evaluation of seismic performance of 3-story 3D one- and two-way steel momentframe structures.” *Earthquake Eng. Struct. Dyn.*, 37, 681–696.

Vamvatsikos, D., and Cornell, C. A. (2002). “Incremental dynamic analysis.” *Earthquake Eng. Struct. Dyn.*, 31(3), 491–514.

Vamvatsikos, D., and Cornell, C. A. (2005a). “Direct estimation of the seismic demand and capacity of multi-degree-of-freedom systems through incremental

dynamic analysis of single degree of freedom approximation.” J. Struct. Eng., 131(4), 589–599.

Villaverde, R. (2007). “Methods to assess the seismic collapse capacity of building structures: State of the art.” J. Struct. Eng., 133(1), 57–66.

Zareian, F., and Krawinkler, H. (2007). “Assessment of probability of collapse and design for collapse safety.” Earthquake Eng. Struct. Dyn., 36, 1901–1914.